Anticancer, photoluminescence and electrochemical properties of structurally characterised two imine derivatives

Gökhan Ceyhan, Muhammet Köse, Mehmet Tümer, İbrahim Demirtaş

PII: S1386-1425(15)00609-5
DOI: http://dx.doi.org/10.1016/j.saa.2015.05.021
Reference: SAA 13688

To appear in: *Spectrochimica Acta Part A: Molecular and Biomolecular Spectroscopy*

Received Date: 8 December 2014
Revised Date: 17 March 2015
Accepted Date: 5 May 2015

Please cite this article as: G. Ceyhan, M. Köse, M. Tümer, İ. Demirtaş, Anticancer, photoluminescence and electrochemical properties of structurally characterised two imine derivatives, *Spectrochimica Acta Part A: Molecular and Biomolecular Spectroscopy* (2015), doi: http://dx.doi.org/10.1016/j.saa.2015.05.021

Anticancer, photoluminescence and electrochemical properties of structurally characterised two imine derivatives

Gökhan Ceyhan[a], Muhammet Köse[a], Mehmet Tümer[a*], İbrahim Demirtaş[b]

[a]*Chemistry Department, K.Maras Sütcü Imam University, 46100, K.Maras, Turkey.*

[b]*Chemistry Department, Çankırı Karatekin University, 18100, Çankırı, Turkey.*

ABSTRACT

Two imine compounds, 4-[(E)-(2-methoxybenzylidene)amino]phenol (L^1) and 4-[(E)-(3,4-dimethoxybenzylidene)amino]phenol (L^2) were synthesized and characterized by the analytical and spectroscopic methods. The electrochemical and photoluminescence properties of the imine compounds L^1 and L^2 were investigated in different solvents. The compounds L^1 and L^2 show different redox processes at some potentials. The molecular structures of two Schiff base compounds are broadly similar, differing principally in the position, the number of metoxy(-OCH_3) groups and dihedral angles between aromatic rings. While the compound L^1 has only one metoxy group located on the *o*-position with respect to the imine bond (C=N), the L^2 contains two metoxy groups on the *p*-*m*-positions with respect to the imine bond. The imine compounds show two or three emission bands in the 619-832 nm range in organic solvents. In the 1.0 x 10^{-3} M concentration, the compounds have the highest excitation and emission bands. The imine compounds L^1 and L^2 were screened for their *in vitro* cytotoxicity on HeLa cell lines using the xCELLigence system (Real Time Cell Analyzer).

Keywords: Schiff base, Anticancer, Electrochemistry, Photoluminescence

***Corresponding author**: Mehmet Tümer
Tel.: +90 344 280 14 44, **Fax:** +90 344 280 13 52,
E-mail address: mtumer@ksu.edu.tr

1. Introduction

Imine compounds (called also Schiff bases) are synthesized from the reaction of aliphatic or aromatic primary amines with aldehydes or ketones. They are nitrogen analogue of an aldehyde or a ketone in which the carbonyl group (CO) has been replaced by an imine (azomethine -C=N-) group. Schiff bases form an important class of the most widely used as organic compounds and has a wide variety of applications in many fields, e.g., biological, inorganic and analytical chemistry. Some of them are the basic units in certain dyes and are also used as liquid crystals. Schiff bases appear to be important intermediates in a number of enzymatic reactions involving interaction of an enzyme with an amino or a carbonyl group of a substrate [1].

Imine compounds, obtained frequently from various of the heterocyclic primary amines, were reported to possess a broad spectrum of pharmacological activities with a wide range of biological properties, development of a new chemotherapeutic imine compounds is now attracting the attention of medicinal chemists [2]. They are known to exhibit a wide variety of potent activities. The pharmacologically useful activities include antibacterial, anticonvulsant, antiinflammatory, anticancer, anti-hypertensive, anti-fungal, antipyretic, antimicrobial, anti-HIV, cytotoxic activity, hypnotic and herbicidal activities [3].

Our research group reported a series of imine compounds and their transition metal complexes as biocidal against bacteria and fungi species [4-10]. The biological effects of these compounds were found to be dose dependent. In our other research, the polydentate Schiff base ligands and their Cu(II) and Cd(II) complexes were synthesised [11]. In this research, the Schiff base complexes of cadmium were found to inhibit the intense chemiluminescence reaction in dimethylsulfoxide (DMSO) solution between luminol and dioxygen in the presence of a strong base. This effect is significantly correlated with the stability constants K_{CdL} of the complexes and the protonation constants K_{OH} of the ligands; it also has no significant association with antibacterial activity. We investigated the antioxidant and anticancer properties of the sterically hindered Schiff base compounds [12-14]. Higher absorbance of the reaction mixture indicated greater reducing power of the Schiff base ligands.

In this study, two imine compounds from the reaction of the 2-methoxy benzaldehyde or 3,4-dimethoxy benzaldehyde with 4-aminophenol in the ethanolic solution were prepared and characterized by the analytical and spectroscopic methods. The compounds were structurally characterized by X-ray diffraction studies. Additionally, electrochemical,

luminescence, antioxidant and anticancer properties of the compounds were investigated. The electrochemical and photoluminescence properties of the imine compounds were investigated in different solvents and concentrations.

2. Experimental

2.1 *Materials and measurements*

All reagents and solvents were of reagent-grade quality and obtained from commercial suppliers (Aldrich or Merck). Elemental analyses (C,H,N) were performed using a LECO CHNS 932. Infrared spectra were obtained using KBr disc (4000-400 cm-1) on a Perkin Elmer Spectrum 100 FT-IR. The electronic spectra in the 200–900 nm range were obtained on a Perkin Elmer Lambda 45 spectrophotometer. Mass spectra of the ligands were recorded on a LC/MS APCI AGILENT 1100 MSD spectrophotometer. ^{1}H and ^{13}C NMR spectra were recorded on a Bruker 400 MHz instrument and TMS was used as an internal standard and DMSO-$_{d6}$ as solvent. The thermal studies of the compounds were performed on a Perkin Elmer STA 6000 simultaneous Thermal Analyzer under nitrogen atmosphere at a heating rate of 10 °C/min.

The single-photon fluorescence spectra of the Schiff base compounds L^1 and L^2 were collected on a Perkin Elmer LS55 luminescence spectrometer. All samples were prepared in spectrophotometric grade solvents and analysed in a 1 cm optical path quartz cuvette. The solutions of ligands (1.0×10^{-3}-1.0×10^{-7} mol L^{-1}) were prepared in DMF solvent. To investigate the solvent effect on the photoluminescence spectra of the ligands, the DMF, DMSO, $CHCl_3$, CH_3OH and C_2H_5OH solutions (1.0×10^{-3} mol L^{-1}) of the compounds were used.

A stock solution of concentrations of 1.0×10^{-3} M and 1.0×10^{-4} M of Schiff base compounds was prepared in DMF for electrochemical studies. Cyclic voltammograms were recorded on a Iviumstat Electrochemical workstation equipped with a low current module (BAS PA–1) recorder. The electrochemical cell was equipped with a BAS glassy carbon working electrode (area 4,6 mm^2), a platinum coil auxiliary electrode and a Ag^+/AgCl reference electrode filled with tetrabutylammonium tetrafloroborate (0.1 M) in DMF and CH_3CN solution and adjusted to 0.00 V vs SCE. Cyclic voltammetric measurements were performed at room temperature in an undivided cell (BAS model C–3 cell stand) with a platinum counter electrode and an Ag^+/AgCl reference electrode (BAS). All potentials are reported with respect to Ag^+/AgCl. The solutions were deoxygenated by passing dry nitrogen

through the solution for 30 min prior to the experiments, and during the experiments the flow was maintained over the solution. Digital simulations were performed using DigiSim 3.0 for windows (BAS, Inc.). Experimental cyclic voltammograms used for the fitting process had the background subtracted and were corrected electronically for ohmic drop. Mettler Toledo MP 220 pH meters was used for the pH measurements using a combined electrode (glass electrode reference electrode) with an accuracy of ±0.05 pH.

Data collection for X-ray crystallography was completed using a Bruker APEX2 CCD diffractometer and data reduction was performed using Bruker SAINT [15]. SHELXTL was used to solve and refine the structures [16].

2.2 *Synthesis of the Schiff base compounds*

The benzaldehyde derivatives (1 mmol; 136 mg 2-methoxy benzaldehyde for L^1 or 166 mg 3,4-dimethoxy benzaldehyde for L^2) in ethanol (20 mL, absolute) and 4-aminophenol (1 mmol, 109 mg) in ethanol (20 mL, absolute) were mixed and refluxed for about 10 h at 80 °C. The color of the solution changed to yellow. After cooling the solution, the resulting precipitate was filtered and washed with cold ethanol. Single crystals of the Schiff base compounds (L^1 and L^2) suitable for X-ray diffraction study were obtained by slow evaporation of the compounds in ethanol. Physical properties and other spectroscopic data are given below.

L^1: ($C_{14}H_{13}NO_2$). Yield: 90%, color: yellow, m.p.: 160 °C. Elemental analyses, found (calcd. %): C, 74.03 (73.99); H, 5.80 (5.77); N, 6.20 (6.16). ^{1}H NMR (DMSO-$_{d6}$, δ (ppm)): 8.64 (s, CH=N, 1H), 7.90-6.30 (m, Ar-H, 8H), 3.80 (s, OCH_3, 3H). ^{13}C NMR (DMSO-$_{d6}$, δ (ppm)): 164.30 (CH=N), 158.20-106.60 (Ar-C), 57.15 (OCH_3). Mass spectrum (LC/MS APCI): m/z 228 $[M+1]^+$ (100%), m/z 229 $[M + 2]^+$ (22%), m/z 213 $[M –CH_3]^+$ (5%). FT-IR: (KBr, cm^{-1}): 3200 ν(O-H), 3010 $\nu(C\text{-}H)_{aromatic}$, 2960 $\nu(C\text{-}H)_{alph}$, 1605 ν(CH=N).

L^2: ($C_{15}H_{15}NO_3$). Yield: 85%, color: yellow, m.p.: 155 °C. Elemental analyses, found (calcd. %): C, 70.05 (70.02); H, 5.90 (5.88); N, 5.40 (5.44). ^{1}H NMR (DMSO-$_{d6}$, δ (ppm)): 9.42 (s, OH, 1H), 8.72 (s, CH=N, 1H), 7.95-6.62 (m, Ar-H, 7H), 3.84, 3.88 (s, OCH_3, 6H). ^{13}C NMR (DMSO-$_{d6}$, δ (ppm)): 163.62 (CH=N), 160.87-98.54 (Ar-C), 56.25, 55.93 (OCH_3). Mass spectrum (LC/MS APCI): m/z 258 $[M+1]^+$ (100%), m/z 259 $[M + 2]^+$ (23%), m/z 120 $[C_7H_6NO]^+$ (48%). FT-IR: (KBr, cm^{-1}): 3077 ν(O-H), 3014 $\nu(C\text{-}H)_{aromatic}$, 2947 $\nu(C\text{-}H)_{alph}$, 1616 ν(CH=N).

2.3 *X-ray structure solution and refinement for the compounds L^1 and L^2*

Data for the compounds L^1 and L^2 were collected at 150(2)K° on a Bruker Apex2 CCD diffractometer using Mo-*Kα* radiation (λ = 0.71073Å). The structures were solved by direct methods and refined on F^2 using all the reflections [15]. All the non-hydrogen atoms were refined using anisotropic atomic displacement parameters and hydrogen atoms bonded to carbon atoms were inserted at calculated positions using a riding model. Hydrogen atoms bonded to oxygen atoms in were located from difference maps and refined with temperature factors riding on the carrier atom. Details of the crystal data and refinement are given Table 1.

2.4 *Anticancer activity studies of the Schiff base compounds*

2.4.1 Preparation of samples

Stock solutions of the samples were prepared in DMSO and diluted with Dulbecco's modified eagle medium (DMEM). DMSO final concentration is below 1% in all tests.

2.4.2 Cell lines and cell culture

HeLa cancer cell lines were grown in Dulbecco's modified eagle medium (DMEM) supplemented with 10% fetal bovine serum (FBS), 2% penicilin streptomycin. The medium was changed twice a week.

2.4.3 Cell proliferation assay

The Real Time Cell Analyzer-Single Plate (RTCA-SP, xCELLigence) instrument (Roche Applied Science, Basel, Switzerland) was used to visualize the antiproliferative effects of the compounds L^1 and L^2 on human cervical cancer (HeLa) cells. RTCA-SP is a combination of four parts: an E-Plate 96, a Single Plate (SP) station that is kept in an incubator and holds the E-Plate 96, an analyzer and a computer with RTCA software. The E-Plate 96 wells have an inner volume of 243±5 μL and their bottoms are coated with golden electrodes. The xCELLigence measures impedance differences set by an operator in order to derive cell index values at time points and impedance differences as well as the cell index values depends on the cell activity at the bottom of the wells. The higher cell index value depends on the higher the cell population growing at the bottom and the greater the spreading of the cells. RTCA allows researchers to analyze cell behavior in a labeling-free cell-based assay and produces a real-time profile of the cells.

The HeLa cell line was cultured in DMEM-HG supplemented with 100 mL L^{-1} heat-inactivated FBS and 20 mL L^{-1} penicillin/streptomycin at 37 °C in a humidified atmosphere of 5% CO_2.

To determine the antiproliferative effects of the synthesised imines, HeLa cells were first detached from the tissue culture flask by the treatment with trypsin/ethylenediaminetetraacetic acid solution. After detachment, the same volume of culture medium was added to this cell suspension and gently mixed. Then the suspension was partitioned into Falcon tubes and centrifuged. Meanwhile, 50 μL of culture medium was added to each well of the E-Plate 96 and left in the hood for 15 min and in the incubator for 15 min to allow the electrodes to equilibrate with the culture medium. After this period, the E-Plate 96 was inserted into the RTCA-SP station and a background measurement was performed. Immediately afterwards, the E-Plate 96 was ejected from the station and 100 μL of cell suspension adjusted to a concentration of 2.5×10^4 HeLa cells per 100 μL^{-1} was added to each well. Three wells were left blank to check if there would be an increase due to the culture medium. The plate was left in the hood for another 30 min for the cells to adhere to the bottom, after which the plate was inserted into the RTCA-SP station and a measurement lasting 80 min was started. After this period, the plate was ejected from the station and plant extracts (in dimethyl sulfoxide (DMSO)/culture medium; the final concentration of DMSO in the wells was less than 10 mL L^{-1}) were added to the wells at three different concentrations (100, 50 and 10 μg mL^{-1}), and the final volume of each well was adjusted to 200 μL with culture medium. Then the plate was connected to the station and a measurement lasting 48 h was started. The measurement was made in triplicate.

2.4.4 Statistical analysis

All experiments were performed in triplicate. The proliferation tests were evaluated as mean±SD of three measurements of cell index values by ANOVA at 1% significance level and compared by Tukey's one-way comparison test for differences using Minitab 14 (Minitab Inc., State College, PA, USA).

3. Results and Discussion

In this manuscript, two imine compounds L^1 and L^2 containing methoxy groups were prepared. These compounds are stable at room temperature without decomposing. They are soluble in polar organic solvents such as, EtOH, MeOH, $CHCl_3$, DMF, DMSO *etc*. and partially soluble in apolar solvents such as, hexane, heptane, toluene etc. The compounds were characterised by the spectroscopic and analytic techniques. Structural characterizations of the synthesised compounds were determined by single crystal X-ray diffraction technique. The proposed structures of the imine compounds are shown in Fig. 1. The imine compounds were purified by the crystallization method. Because, if their purification is performed by the colon technique, the compounds may be decompose as hydrolysis. In such cases, it is better to purify the Schiff bases by re-crystallization. A problem in studying with the Schiff bases of the aromatic hydroxycarbonyls derives essentially, even in neutral solutions several of species may be appear. Additionally to enolimines, hemiacetals and their hydrolysis products, tautomeric species, may also formed, like keto-amines or cyclic diamines formed from mono Schiff bases of diamines. This truth is often omitted, although it must be taken account of when protonation equlibria are analysed [17].

In order to clarify the structures of the Schiff bases (L^1 and L^2), their $^1H(^{13}C)$-NMR spectra were investigated and obtained data are given in the experimental section. The $^1H(^{13}C)$-NMR spectra of the imine compound L^2 are given in Figs. 2a-d. In the ^1H-NMR spectrum of the imine compound L^2, the broad band at 9.42 ppm can be attributed to the hydrogen atom of the OH group. In the ^1H-NMR spectra of the imine compounds L^1 and L^2, the singlets at 8.64 and 8.72 ppm can be attributed to the protons of the azomethine groups. The aromatic ring protons are shown in the 7.95-6.30 ppm range as multiplet. The signals of the methoxy groups on the benzene rings are shown in the 3.88-3.80 ppm range as singlet signals. In their ^{13}C-NMR spectra, the signals at 164.30 and 163.62 ppm may be assigned to the carbon atom of the azomethine group. Aromatic carbon atoms are shown in the 160.87-98.54 ppm range. The signals in the 57.15-55.93 ppm range can be attributed to the methoxy carbon atoms.

The infrared spectral data of the compounds are given in the experimental section. In the FT-IR spectra of the imine compounds (L^1 and L^2), the broad bands in the 3200 and 3070 cm^{-1} may be assigned to the ν(O-H) vibrations. The vibration signals at 3010 and 3014 cm^{-1} can be attributed to the aromatic C-H strechings. The bands at 2960 and 2947 cm^{-1} may be assigned to the $\nu(C\text{-}H)_{alph}$ vibrations. The azomethine group [ν(CH=N)] vibrations are shown at 1605 and 1616 cm^{-1}.

The most useful techniques for investigating the tautomeric forms (Fig. 3) of the ligands are UV and NMR spectroscopies, whereas IR seems to be of limited value here because the locations of the ν(C-O) and ν(C=O) stretching frequencies in the spectra are obscured by the abundance of aromatic skeletal modes. The CH=N and OH groups of the enolimine–ketoamine tautomers are capable of forming hydrogen bonds with suitable solvents. Due to the stronger hydrogen bond donor ability of the OH groups compared with that of the CH=N group, the formation of hydrogen bonds mainly with chloroform and ethanol solvents should stabilize the enol-imine form, whereas the basic ketoamine form should be more stabilized in solvents such as toluene and heptane. It has been shown by electronic spectroscopy that the equilibrium in less polar and non-polar solvents is shifted towards the ketoamine form. On the other hand, hydrogen bond acceptor solvents favour the enolimine form due to hydrogen bonding [18]. In order to investigate the solvent effect, the spectra of the compounds were taken in the polar and apolar organic solvents. These solvents are MeOH, EtOH, DMF, DMSO CH_2Cl_2, $CHCl_3$, n-hexane, n-heptane, cyclohexane and tolüene solutions. The electronic spectra of the compounds L^1 and L^2 in the 1 x 10^{-3} M concentration and in the different solvents are shown in Figs. 4a-d. In addition, the obtained data from the electronic absorption studies are given in the Table 1. The imine compounds show different tautomeric forms depending on the solvent polarity. In polar organic solvents, the imine compounds show the bands in the 371-291 nm range and this bands may be attributed to the n-π* transitions [19]. In this region, the compounds have the bands with maximum intensity in the methanol solution. The bands with maximum intensity in the 208-273 nm range can be assigned to the benzenoid transitions (π-π* and δ-δ*). In the non-polar organic solvents, the n-π* transitions of the imine compounds are shown in the 515-292 nm range. The n-π* transition of the imine compound L^1 shifted to the longer wavelength in the n-heptane solution. The π-π* and δ-δ* transitions were shown in the 289-212 nm range.

Single crystals suitable for single crystal X-ray diffraction study were obtained from slow evaporation of the ethanol solution of the imine compounds L^1 and L^2. Molecular structures of the imines L^1 and L^2 are shown in Figs. 5 and 6. The molecular structures of two imine compounds are broadly similar, differing principally in the position, the number of methoxy (-OCH_3) groups and dihedral angles between aromatic rings. While the compound L^1 has only one methoxy group located on the *o*-position with respect to the imine bond (C=N), the compound L^2 contains two methoxy groups on the *m-p*-positions with respect to the imine bond. For the imine compounds L^1 and L^2, all bond lengths and angles in the phenyl

rings have normal *Csp2–Csp2* values and are in the expected ranges. The crystallograhic data for the imine compounds L^1 and L^2 are given in Table 2. The C=N distances in both compounds are within a typical C=N double bond character. The compounds show intermolecular phenol-imine hydrogen bonds. Hydrogen bond parameters for the imines L^1 and L^2 are given in Tables 3 and 4, respectively.

In the structure of the imine L^1, the asymmetric unit contains two independent Schiff base molecules (molecule A and B) differing in the dihedral angles between two aromatic rings. The dihedral angles between two aromatic rings are 46.74(4) and 7.92(5)º for molecules A and B, respectively. In the structure of the imine L^1, four molecules are assembled by intermolecular hydrogen bonds forming a supramolecular 28-membered ring (Fig. 7). Molecular packing of the imine L^1 is determined by OH···N and C-H···O hydrogen bondings (Table 3). Packing diagram of L^1 is shown in Fig. 8.

The asymmetric unit of L^2 contains four independent imine molecules (A-D). All four molecules exhibit similar bond length and angles, however, the dihedral angle between two aromatic rings in each molecule is different from each other. The dihedral angles between aromatic rings in four molecules (A-D) of the imine L^2 are 21.34(9), 10.03(9), 71.94(6) and 38.04(8)º for molecules (A-D), respectively. Overlay of four different conformers emphasising the twist in the phenol ring is shown in Fig. 9. The molecules of the imine L^2 are connected *via* phenol-imine (OH···N) intermolecular hydrogen bonding resulting in a hydrogen bonded chain Fig. 10.

3.1 *The effect of different solvent and concentration on the photoluminescence properties of the imine compounds L^1 and L^2*

In order to determine the effect of the solvent polarity, the photoluminescence properties of the imine compounds L^1 and L^2 were investigated in the DMF, DMSO, $CHCl_3$, CH_3OH and C_2H_5OH solvents. The emission and excitation spectra of the Schiff base compounds L^1 and L^2 in the $CHCl_3$ and C_2H_5OH solvents are shown in Figs. 11a-d and the obtained data are given in Tables 5 and 6. Dielectric constant order of the solvents is DMSO>DMF>CH_3OH>C_2H_5OH>$CHCl_3$. In the excitation spectra of the imine compound L^1 in the DMF and DMSO solvents, two bands were shown in the 320-476 nm range. On the other hand, in the $CHCl_3$, CH_3OH and C_2H_5OH solvents, only one band was shown in the 395-431 nm range. While the excitation band shifted to the shorter wavelenght in DMSO solution, the band shifted to the longer wavelenght value in DMF solution. In the excitation spectra of the imine compound L^2, the compund has two excitation bands in the 245-400 nm

range in the $CHCl_3$ and CH_3OH solvents. In the C_2H_5OH solvent, the compound L^2 has three excitation bands in the 239-363 nm range. In the DMF and DMSO solutions, only one band was shown in the 407-417 nm range. The excitation bands of the imine compound L^1 shifted to the longer wavelenghts compared to the imine compound L^2.

The emission spectra of the compounds L^1 and L^2 show two or three emission bands in the 619–832 nm range in the DMF, DMSO, $CHCl_3$, CH_3OH and C_2H_5OH solutions. The emission peaks of the compound L^1 shifted to the longer wavelengths. The photoluminescence emission peaks of the imine compounds apparently produce red shift with the introduction of the electron donating groups. The introduction of the electron donating groups by mesomeric and inductive effects causes the fluorescence characteristic emission peaks of the imine compounds to the slightly red shift. The reason is that the electron density of the phenyl ring is increased with the δ-π hyper conjugation effect. The Schiff bases with methoxy substituents possess p-π conjugation that can increase their photoluminescence emission intensity. As the imine compound L^2 have p-methoxy substitute group, it shows a good conjugation and rigid planar structure. It may be that the extended π-conjugation would induce an excited state resonance contribution of the methoxy groups to the benzene rings in the increased polarity.

In order to investigate the effects of the concentration on the photoluminescence properties of the imine compounds L^1 and L^2, the solutions in $1.0x10^{-3}$-$1.0x10^{-7}$ M range in DMF, DMSO, $CHCl_3$, CH_3OH and C_2H_5OH solutions were used. In the spectra of the compounds, the emission peaks did not shift to the shorter or longer wavelenghts (SW) from $1.0x10^{-3}$ M to $1.0x10^{-7}$ M concentration. However, the intensity of the absorption bands were decreased towards to lower concentrations. This situation occur due to the lesser substance quantity in lower concentrations. Similar properties were also shown for the excitation peaks.

3.2 *The electrochemical properties of the compounds L^1 and L^2*

Electrochemical properties of the imine compounds (L^1 and L^2) were studied in CH_3CN and DMF - 0.1 M NBu_4BF_4 as supporting electrolyte at 298 K. In order to study the effects of the solution concentration and the scan rates, two different concentrations ($1.0x10^{-3}$ and $1.0x10^{-4}$ M) and the scan rates (100, 250, 500, 750 and 1000 mV/s) were used against an internal ferrocence-ferrocenium standard. The obtained data are given in Table 7. The electrochemical curves of the compounds L^1 and L^2 in DMF and CH_3CN solutions are shown in Figs. 12a-d.

In the $1.0x10^{-3}$ M CH_3CN solution, the imine compound L^1 shows three anodic peak potentials in the -0.79-1.13 V range at all scan rates. In the same solution, the compound has two cathodic peaks in the -0.09-0.74 V range. In DMF solution, while the compound has two anodic peaks in the -0.85-0.65 V range, the compound has three cathodic peaks in the -0.94-0.89 V range. The anodic peaks in the 1.09-1.13 V range in the CH_3CN solution of the compound L^1 were disappeared in DMF solution. On the other hand, the cathodic peaks in the -0.90-0.94 V range were determined. In the $1x10^{-4}$ M CH_3CN solution, the compound L^1 has two anodic peaks in the -0.49-1.15 V range. But, this compound has three cathodic peaks in the -1.06-0.61 V range. In DMF solution, the compound L^1 has two anodic and cathodic peaks in the -0.58-0.30 and -0.79-0.18 V range, respectively. From the obtained data for the imine compound, the scanning rate, solvent polarity and solution concentration were effective on the redox processes. At all scan rates, the redox processes for the imine compound L^1 are either quasi-reversible or irreversible events (Fig. 13a).

In the $1.0x10^{-3}$ M CH_3CN solution, the imine compound L^2 shows three irreversible anodic peak potentials in the -0.64-1.15 V range at all scan rates. But, the imine has two irreversible cathodic redox processes in the -1.16-0.55 V range. In DMF solution, the imine L^2 has three piece anodic and cathodic peaks in the -0.76-0.67 and -0.76-0.80 V range, respectively. At all scan rates, the redox processes are reversible (Fig. 13b). On the other hand, in the $1x10^{-4}$ M CH_3CN solution, the imine compound L^2 has three irreversible anodic and two cathodic peaks in the -0.56-1.09 and -0.15-0.51 V range, respectively. As distinct from this, in DMF solution, the imine compound L^2 has reversible three anodic and cathodic redox potentials in the -0.49-1.27 and -0.69-1.0 V range, respectively. In the reversible redox process, the Schiff base compounds have been converted to the keto-amine forms [20]. In this process, the oxygen atoms of the methoxy groups of the organic compounds transfer the electrons to the benzenoid rings and then to the nitrogen atoms by the resonance. This process occurs as the reversible. While the compound L^1 has only one methoxy group (*ortho* position on the benzene ring), the other compound L^2 have two methoxy groups (*meta* and *para* positions on the benzene ring). Although the methoxy groups decrease the electron density of the benzenoid rings by the inductive effect, the electron density increase by the mesomeric effect. Electron donating groups to the benzene rings shift the potentials from the positive to negative regions. As a result, the obtained anodic and cathodic data in the CH_3CN shifted to the more negative regions than in DMF solution.

3.3 *The antiproliferative activities of compounds L^1 and L^2*

Figure 11a-b shows the results of xCELLigence real-time monitoring of the proliferation of HeLa cells treated with L^1 and L^2. The cell index measurements indicated that the anticancer activities of synthesised imine derivatives are similar (Figs. 14a,b) except for slight differences in concentrations 50 and 100 µM which are higher activities. The antiproliferative activities of the compounds L^1 and L^2 were very weak to compare with concentrations of 10 µM with 50 and 100 µM. However, these compounds have remarkable activities aganist HeLa cell line in between 10 and 50 µM. According to the recent study, where a new Schiff base (*N*-3,4-dihydroxybenzylidene) ferroceneamine showed an excellent biological activity against the HeLa cancer cell line [21], the hydroxy groups play an important role in anticancer activitiy [22]. The hydroxy and methoxy-substituted Schiff bases have received considerable attention due to their potential anticancer activity. While the compound L^1 has one methoxy group on the *ortho* position of the benzenoid ring, the other compound L^2 has two methoxy groups on the *meta* and *para* position of the benzenoid ring. The methoxy groups give the electron to the aromatic rings by the mesomeric effect. But, the compound L^1 has the higher antiproliferative activity than the L^2. On the other hand, the compounds have only one imine group and this group has an impact on anticancer activity. This showed that different structural requirements exhibit selectivity against different cancer cell lines. In addition, the activity of the compounds L^1 and L^2 have increased in dose-depended manner from 10 to 50 µM. The antiproliferative activity of compound L^1 was more effective than the compound L^2 at 100 and 50 µM aganist HeLa cell line. In the light of the results, it can be suggested that the compounds L^1 and L^2 could be developed as an anticancer drug.

Conclusion

In this work, we synthesized two imine compounds L^1 and L^2 containing methoxy groups and characterized by the analytical, spectroscopic and X-ray techniques. The photoluminescence and electrochemical properties of the compounds were investigated. The compounds L^1 and L^2 show the emission bands at the higher wavelenghts. In addition, the compounds indicate three emission bands. In the electrochemical studies, the compounds showed reversible redox processes at the some scan rates. The molecular structures of two imine compounds are broadly similar, differing principally in the position, the number of methoxy ($-OCH_3$) groups and dihedral angles between aromatic rings. While the compound L^1 has only one methoxy group located on the *o*-position with respect to the imine bond (C=N), the compound L^2

contains two methoxy groups on the *m-p*-positions with respect to the imine bond. The compounds L^2 and L^1 showed higher anticancer activities at higher concentrations. This situation may be due to methoxy groups on the benzenoid rings of the imine compounds.

Supplementary Information

CCDC numbers 1034582 and 1034583 contain the supplementary crystallographic data for L^1 and L^2, respectively. Bond lenghts and angles of the compounds were given in Supplementary Information. These data can be obtained free of charge *via* www.ccdc.cam.ac.uk/data_request/cif, by e-mailing data_request@ccdc.cam.ac.uk, or by contacting The Cambridge Crystallographic Data Centre 12 Union Road Cambridge CB2 1EZ, UK Fax: +44(0)1223-336033.

Acknowledgments: We are grateful to The Scientific & Technological Research Council of Turkey (TUBITAK) (Project number:109T071) for the support of this research. The authors are also grateful to Prof. Dr. Vickie McKee and the Department of Chemistry, Loughborough University for X-ray data collection.

REFERENCES

[1] M. Amanullah, S. K. Sadozai, W. Rehman, Z. Hassan, A. Rauf, M. Iqbal, African J. Biotech. 10 (2011) 209.

[2] B. S. Kumar, K. G. Parthiban, Asian J. Pharm. Clin. Res. 4 (2011) 137.

[3] N. Shahabadi, S. Kashanian, F. Darabi, Eur. J. Med. Chem. 45 (2010) 4239.

[4] M. Tümer, D. Ekinci, F. Tümer, A. Bulut, Spectrochimica Acta Part A, 67 (2007) 916– ?.

[5] M. Tümer, J Coord. Chem., 60(19) (2007) 2051.

[6] M. Tümer, H. Köksal, S. Serin, M. Dığrak, Transition Met. Chem., 24 (1) (1999) 13-17.

[7] M. Tümer, E. Akgün, S. Toroğlu, A. Kayraldız, L. Dönbak, J Coord. Chem., 61(58) (2008) 2935.

[8] M. Dolaz, V. McKee, S. Uruş, N. Demir, A.E. Şabik, A. Gölcü, M. Tümer, Spectrochim Acta Part A, 76(2), (2010) 174-181.

[9] M. Dolaz, V. McKee, A. Gölcü, M. Tümer, Current Org. Chem., 14 (2010) 281-288.

[10] M. Dolaz, V. McKee, A. Gölcü, M. Tümer, Spectrochim Acta Part A, 71 (2009) 1648-1654.

[11] A. Gölcü, M. Tümer, H. Demirelli, R. A. Wheatley, Inorg. Chim. Acta, 358 (2005) 1785–1797.

[12] G. Ceyhan, C. Çelik, S. Uruş, İ. Demirtaş, M. Elmastaş, M. Tümer, Spectrochimica Acta Part A, 81 (2011) 184– 198.

[13] G. Ceyhan, M. Köse, M. Tümer, I. Demirtaş, A.Ş. Yağlioğlu, V. McKee, J. of Lumin., 143 (2013) 623–634.

[14] M. Köse, G. Ceyhan, M. Tümer, I. Demirtaş, I. Gönül, V. McKee, Spectrochimica Acta Part A, 137 (2015) 477-485.

[15] G.M. Sheldrick (2008) Acta Cryst A64:112.

[16] Bruker (1998). APEX2 and SAINT Bruker AXS Inc.

[17] M.S. Blois, Nature 26 (1958) 1199–1200.

[18] M. Dolaz, M. Tümer, Transition Met. Chem., 29, (2004) 528–536.

[19] H. Köksal, M. Dolaz, M. Tümer, S. Serin, Synth. React. Inorg. Met.-Org. Chem., 31(7) (2001) 1141–1162.

[20] M. Tümer, J Coord. Chem., 60(19) (2007) 2051-2065.

[21] V. M. Jiménez-Pérez, B. M. Muñoz-Flores, L. M. Blanco Jerez, A. Gómez, L. D. Rangel, R. Chan-Navarro, N. Waksman, R. Ramírez-Durón, Int. J. Electrochem. Sci., 9 (2014) 7431 - 7445

[22] W. Chen, W. Ou, L. Wang, Y. Hao, J. Cheng, J. Li, Y. N. Liu, Dalton Trans, 42 (2013) 15678

Figure captions

Fig. 1. Proposed structures of the synthesized imine compounds.

Fig. 2a-d. $^{1}H(^{13}C)$-NMR (a) , HMBC (b), HETCOR (c) and TOSCY (d) spectra of the imine compound L^2.

Fig. 3. Tautomeric forms of the imine compounds L^1 (a) and L^2 (b) in the polar and non-polar organic solvents.

Figs. 4a-d. Absorption spectra of the imine compounds L^1 and L^2 in the polar and non-polar organic solvents.

Fig. 5. Molecular structure of the compound L^1 with atom numbering. Intra-molecular hydrogen bonding (OH$\cdots$N) is shown as dashed lines.

Fig. 6. Molecular structure of the compound L^2. Hydrogen atoms are omitted for clarity. Intra-molecular hydrogen bonds (OH$\cdots$N) are shown as dashed lines

Fig. 7. Hydrogen bonded 28 membered macrocyclic in the imine L^1, hydrogen atoms bonded to carbon atoms are not shown for clarity.

Fig. 8. Packing plot of the imine L^1 viewing down c axis, hydrogen bonds are shown as dash lines and hydrogen atoms are omitted for clarity.

Fig. 9. Overlay of four independent molecules in the imine L^2, emphasising the twist in the phenol ring. Hydrogen atoms are omitted for clarity.

Fig. 10. Packing diagram of the imine L^2 showing hydrogen bond chain. Hydrogen atoms are omitted for clarity.

Figs. 11a-d. Photoluminescence (excitation and emission) spectra of the imine compounds L^1 and L^2 in different concentration and solvents.

Figs. 12a-d. CV curves of the imine compounds L^1 and L^2 in different concentrations and solvents in the 100-1000 mV/s range.

Figs. 13a,b. The proposed redox mechanism for the imine compounds L^1 (a) and L^2 (b) in the solution media.

Figs. 14a,b. Anticancer activities of the imine compounds L^1 and L^2.

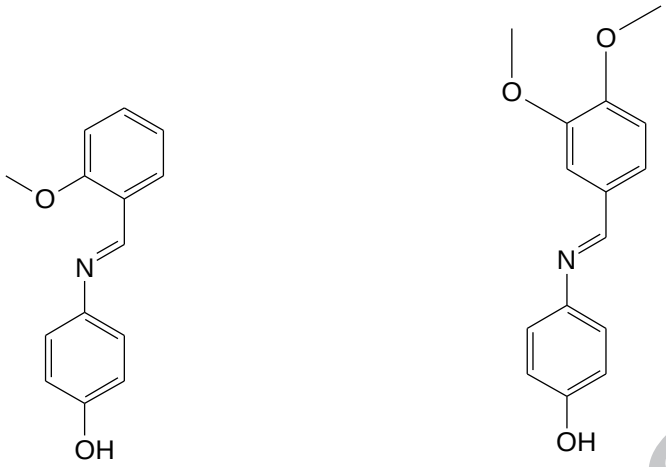

L^1 L^2

Fig. 1. The proposed structures of the synthesized imine compounds L^1 and L^2.

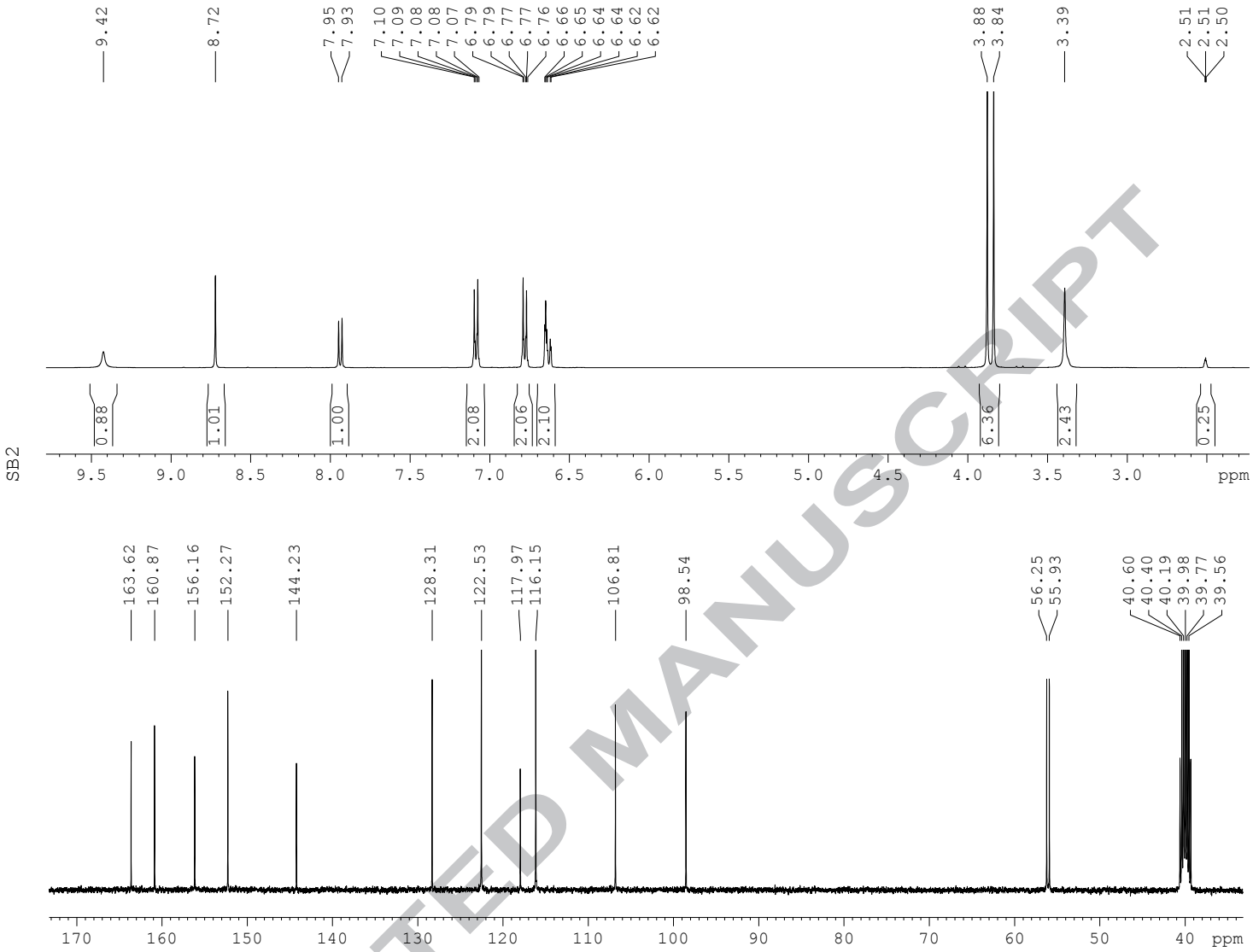

a) $^{1}H(^{13}C)$-NMR

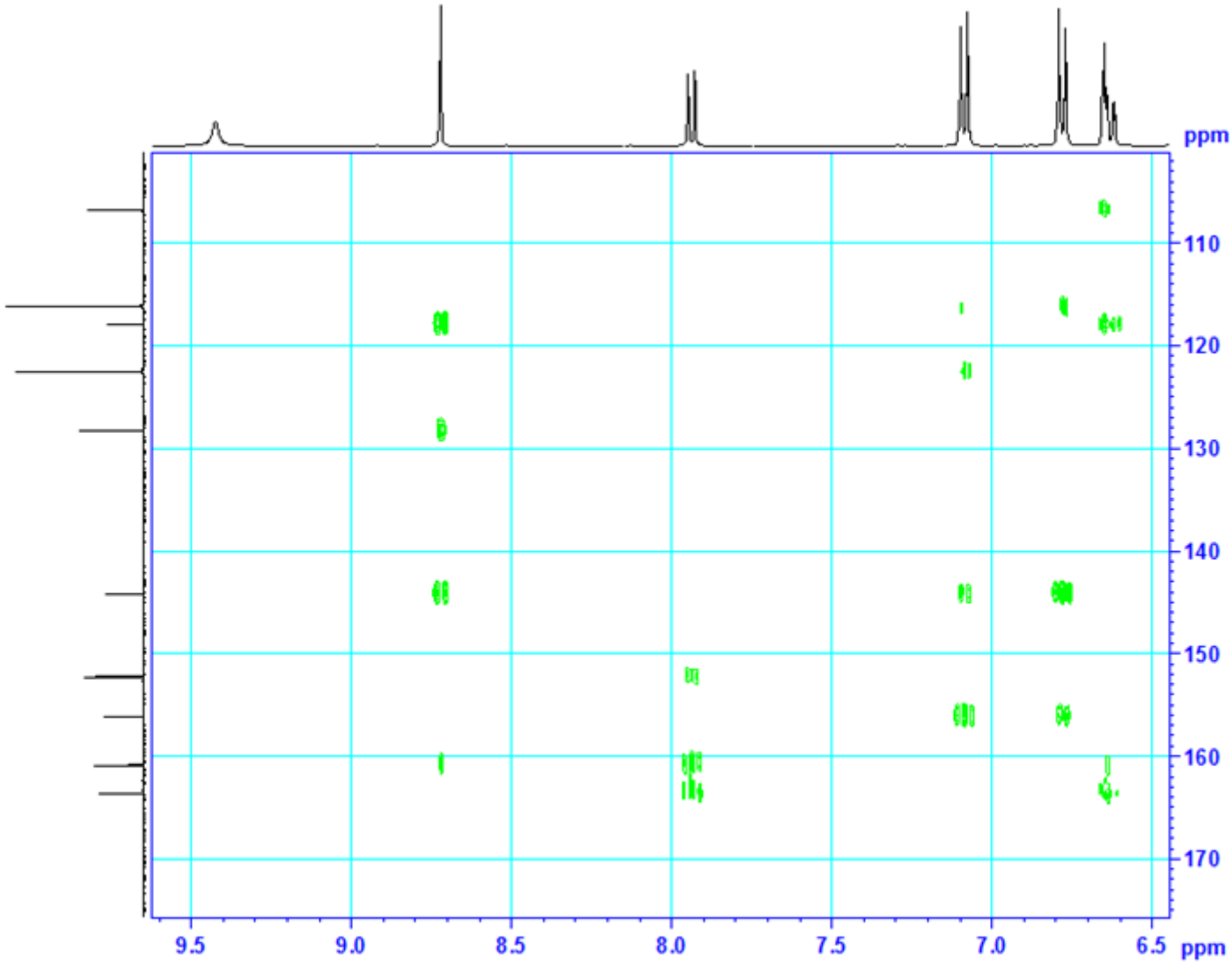

b) HMBC

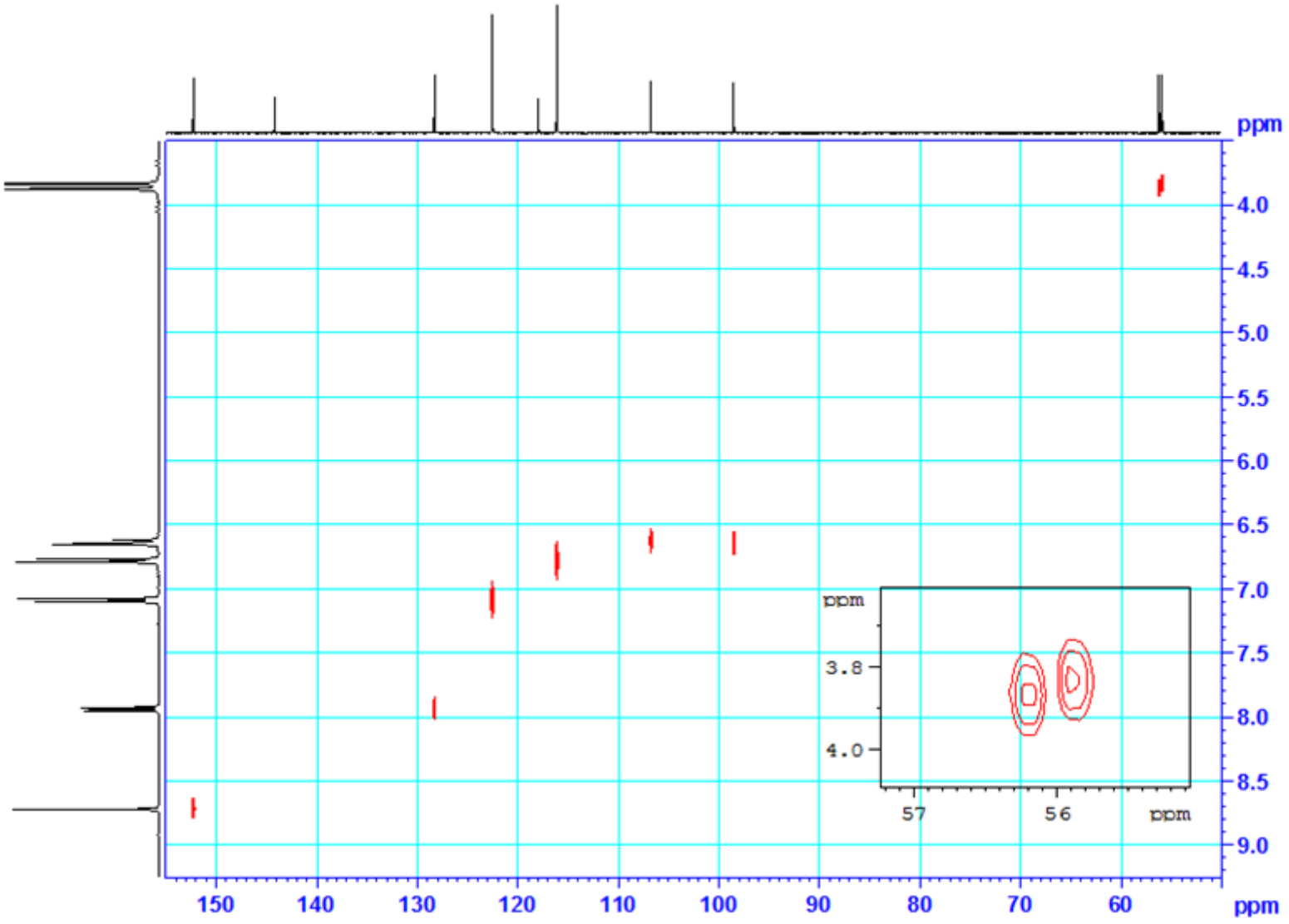
ppm
4.0
4.5
5.0
5.5
6.0
6.5
7.0
7.5
8.0
8.5
9.0
150
140
130
120
110
100
90
80
70
60
ppm
ppm
3.8
4.0
57
56
ppm

c) HETCOR

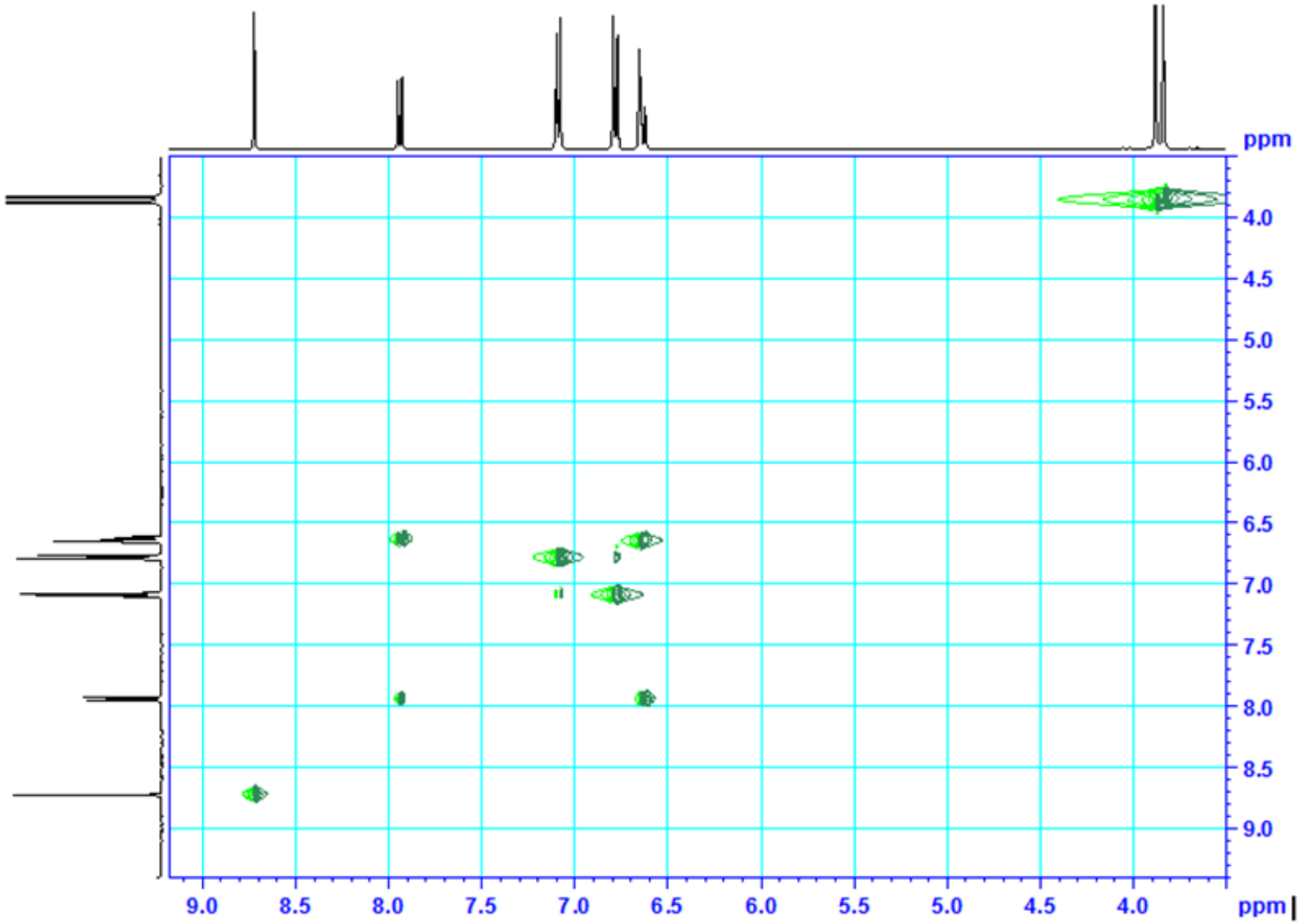

d) TOCSY

Figs. 2a-d. $^{1}H(^{13}C)$-NMR (a) , HMBC (b), HETCOR (c) and TOSCY (d) spectra of the imine compound L^{2}.

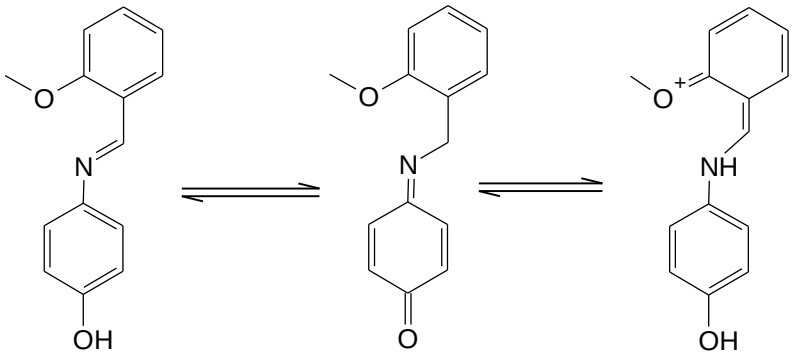

enol-imine keto-imine keto-amine

a)

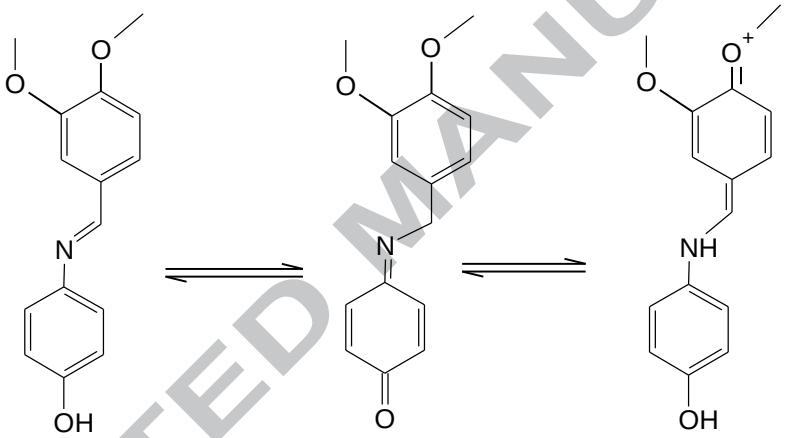

enol-imine keto-imine keto-amine

b)

Fig. 3. Tautomeric forms of the imine compounds L^1 (a) and L^2 (b) in the polar and non-polar organic solvents.

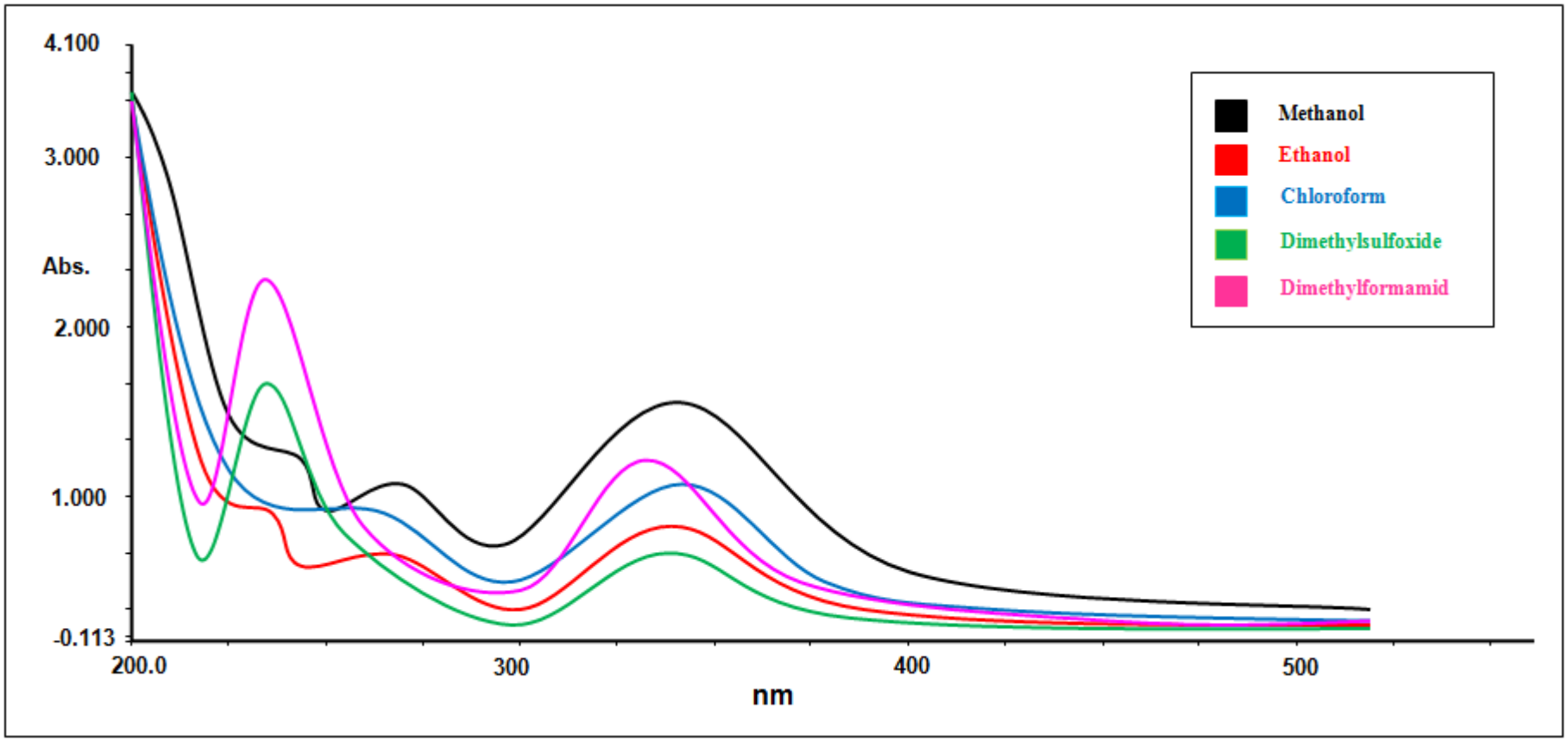

a) L^1

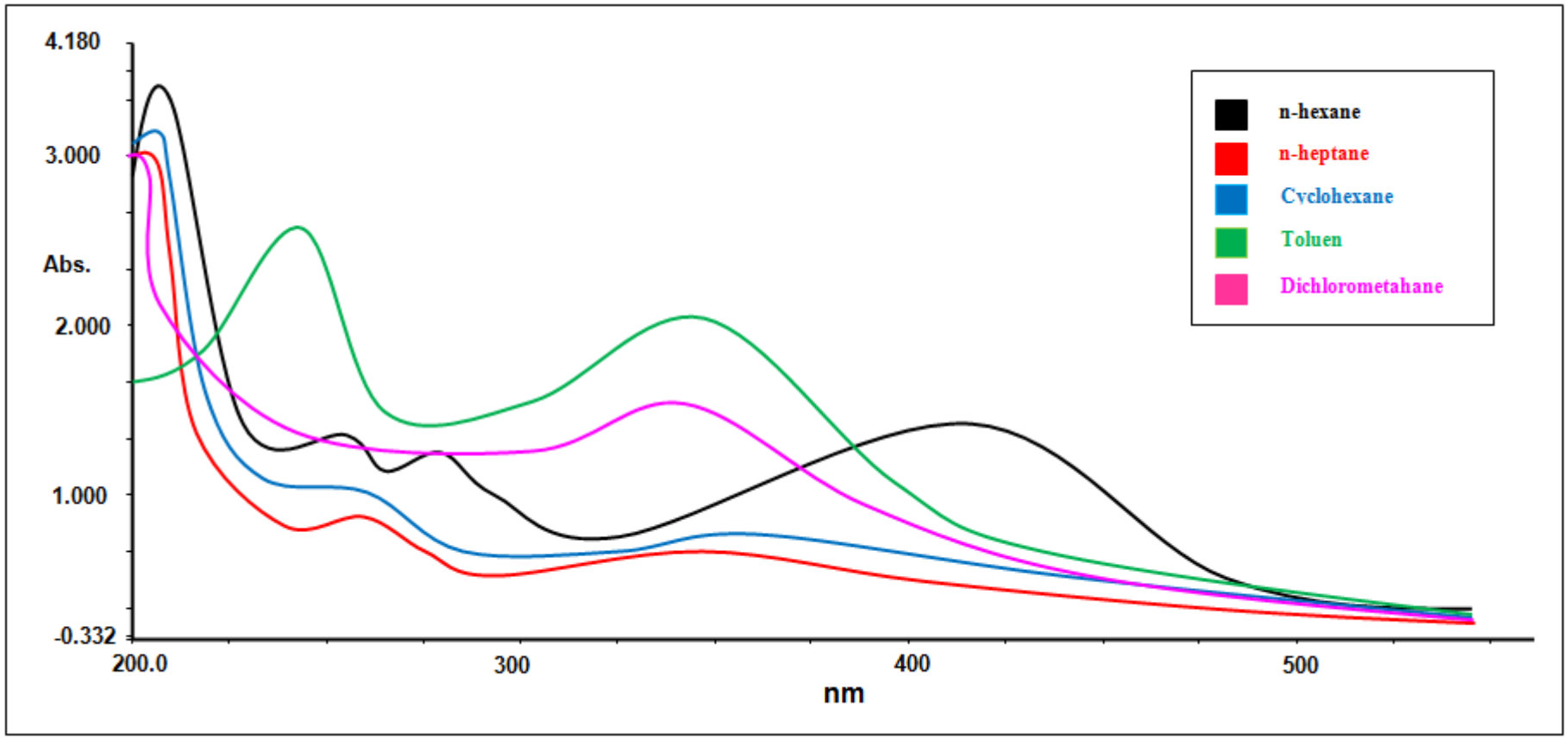

b) L^1

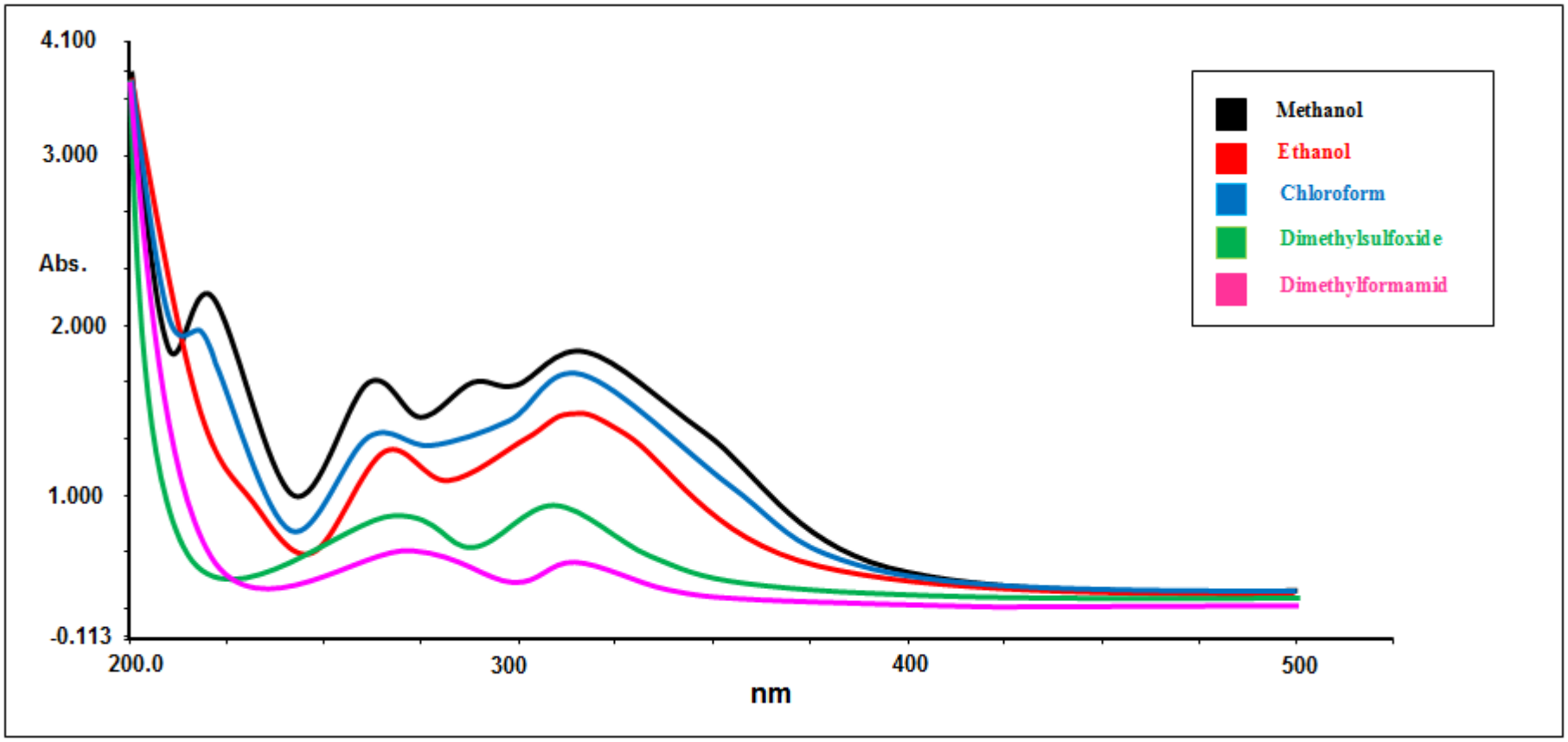

c) L^2

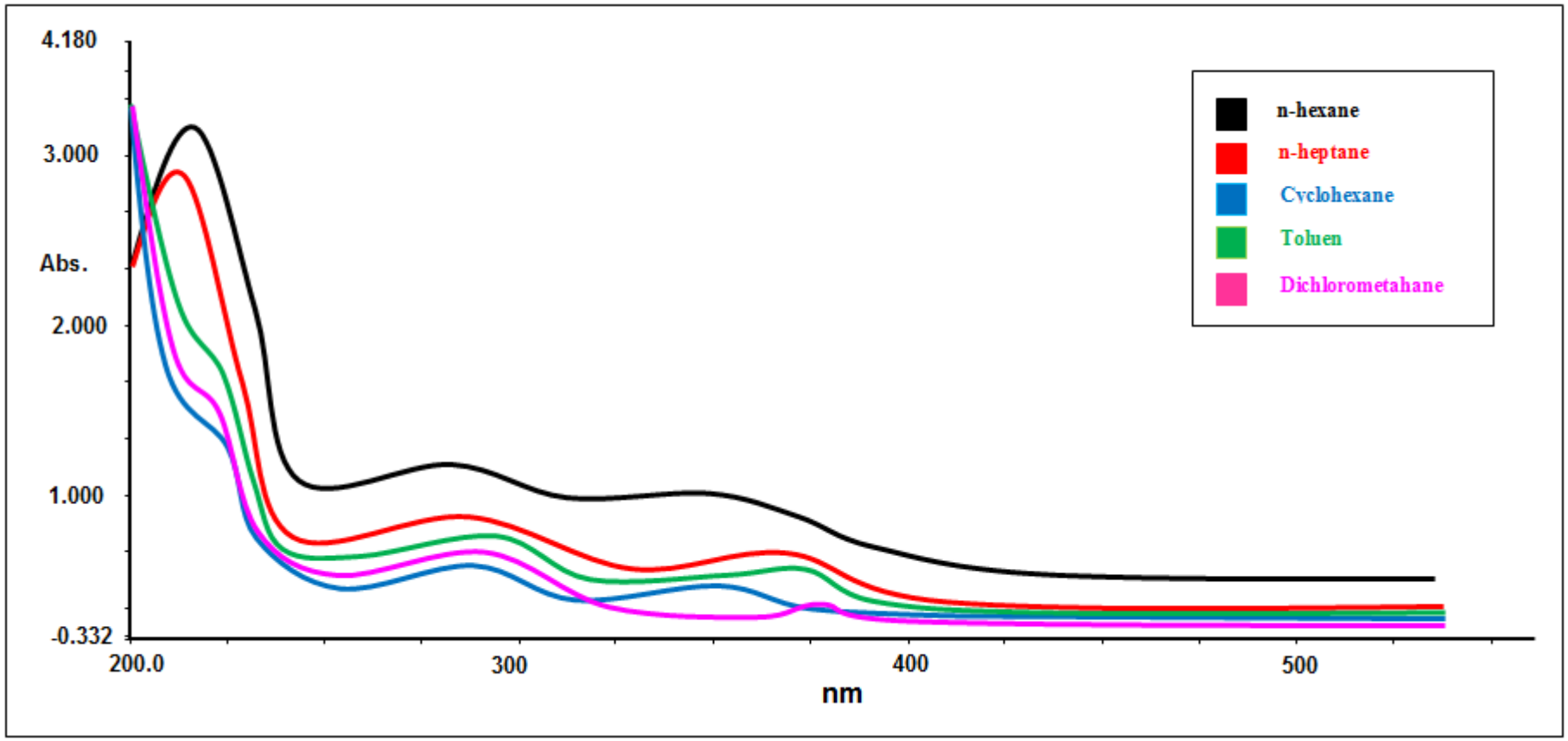

d) L^2

Figs. 4a-d. Absorption spectra of the imine compounds L^1 and L^2 in the polar and non-polar organic solvents.

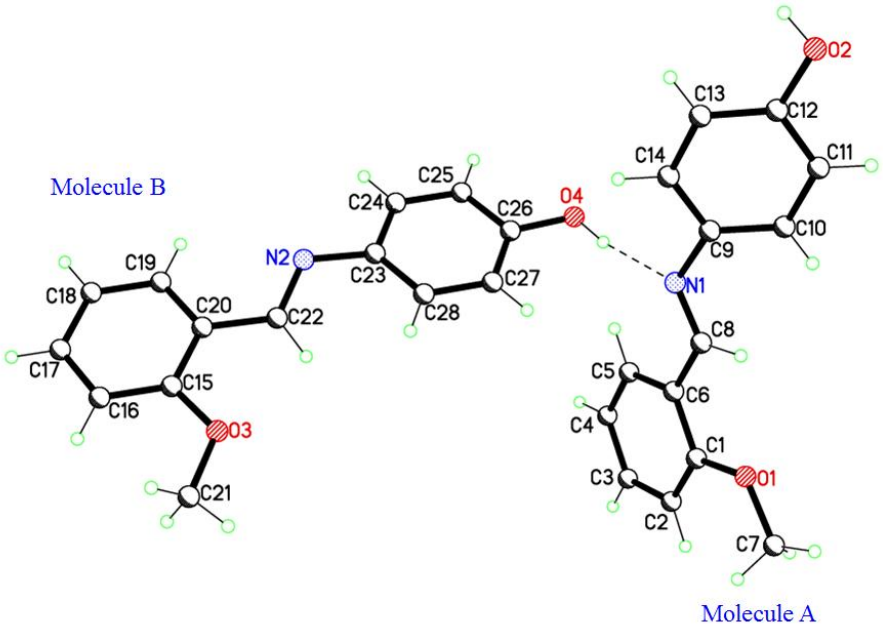

Fig. 5. Molecular structure of the compound L^1 with atom numbering. Intra-molecular hydrogen bonding (OH···N) is shown as dashed lines.

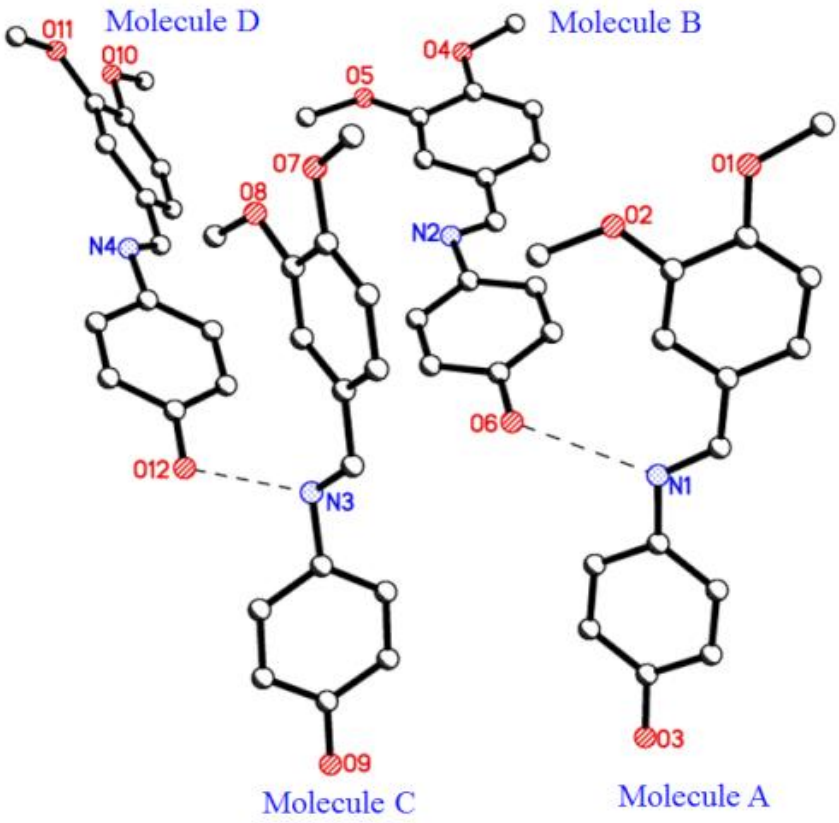

Fig. 6. Molecular structure of the compound L^2. Hydrogen atoms are omitted for clarity. Intra-molecular hydrogen bonds (OH⋯N) are shown as dashed lines.

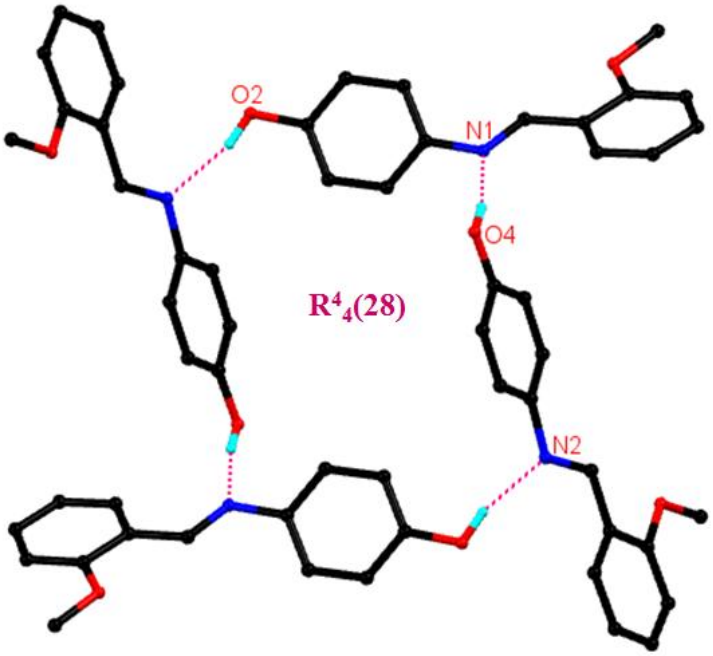

Fig. 7. Hydrogen bonded 28 membered macrocyclic in the imine L^1, hydrogen atoms bonded to carbon atoms are not shown for clarity.

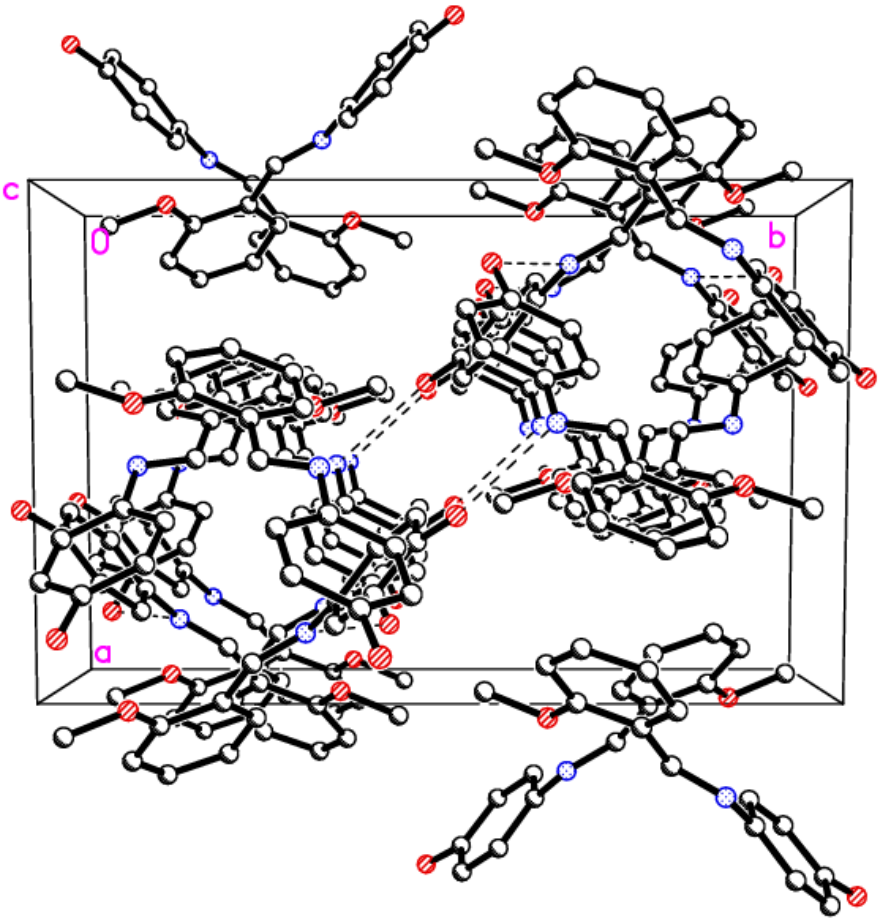

Fig. 8. Packing plot of the imine L^1 viewing down c axis, hydrogen bonds are shown as dash lines and hydrogen atoms are omitted for clarity.

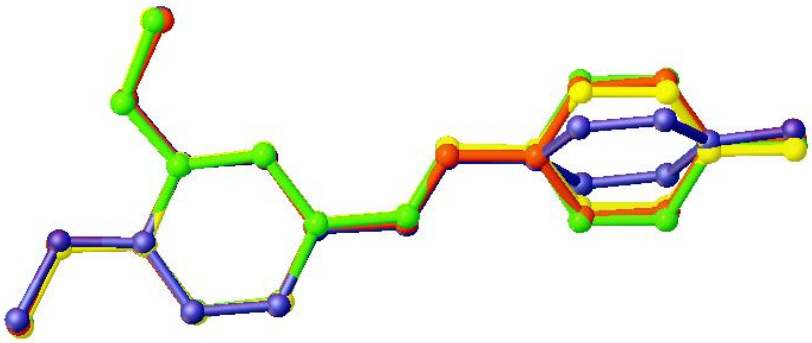

Fig. 9. Overlay of four independent molecules in the imine L^2, emphasising the twist in the phenol ring. Hydrogen atoms are omitted for clarity.

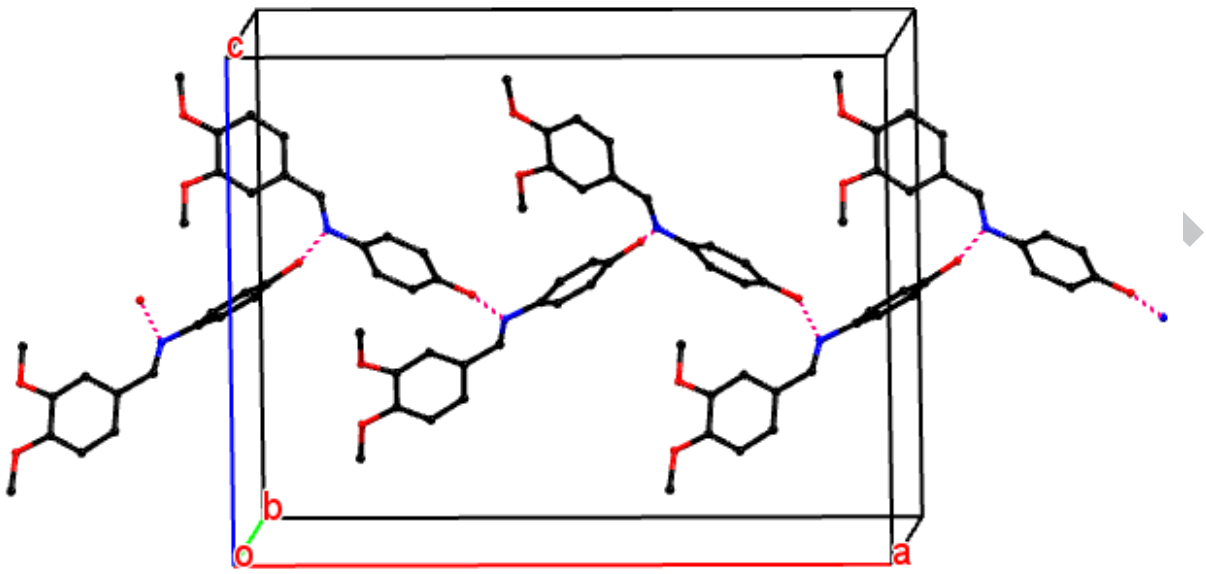

Fig. 10. Packing diagram of the imine L^2 showing hydrogen bond chain. Hydrogen atoms are omitted for clarity.

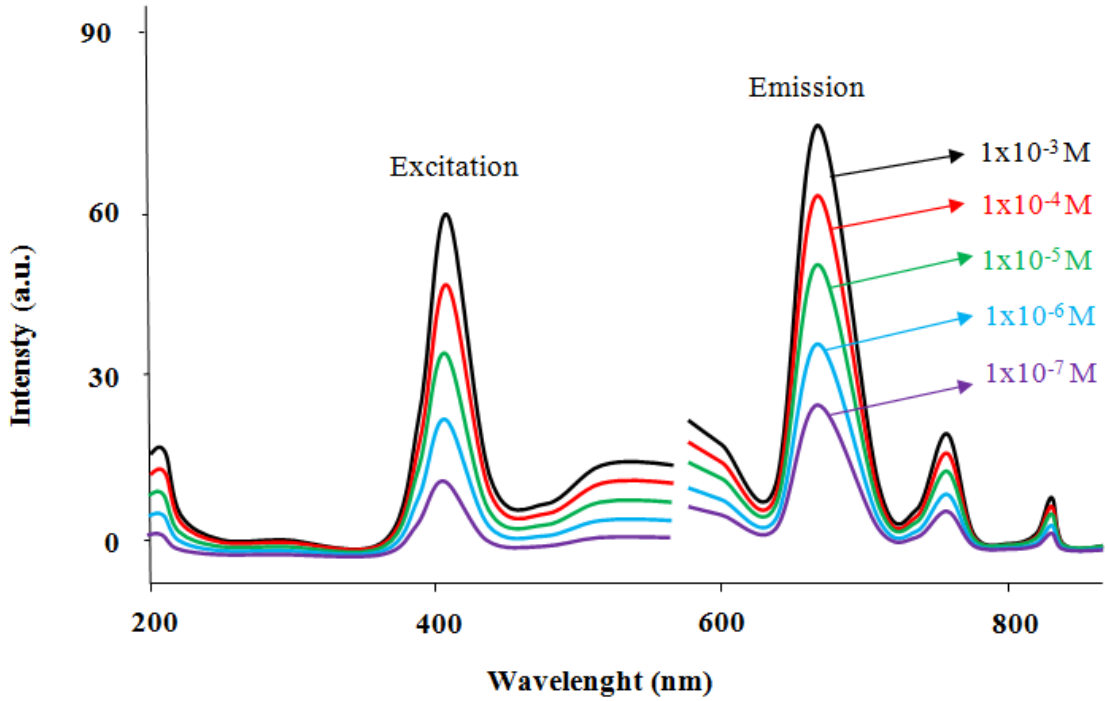

a) L^1 ($CHCl_3$)

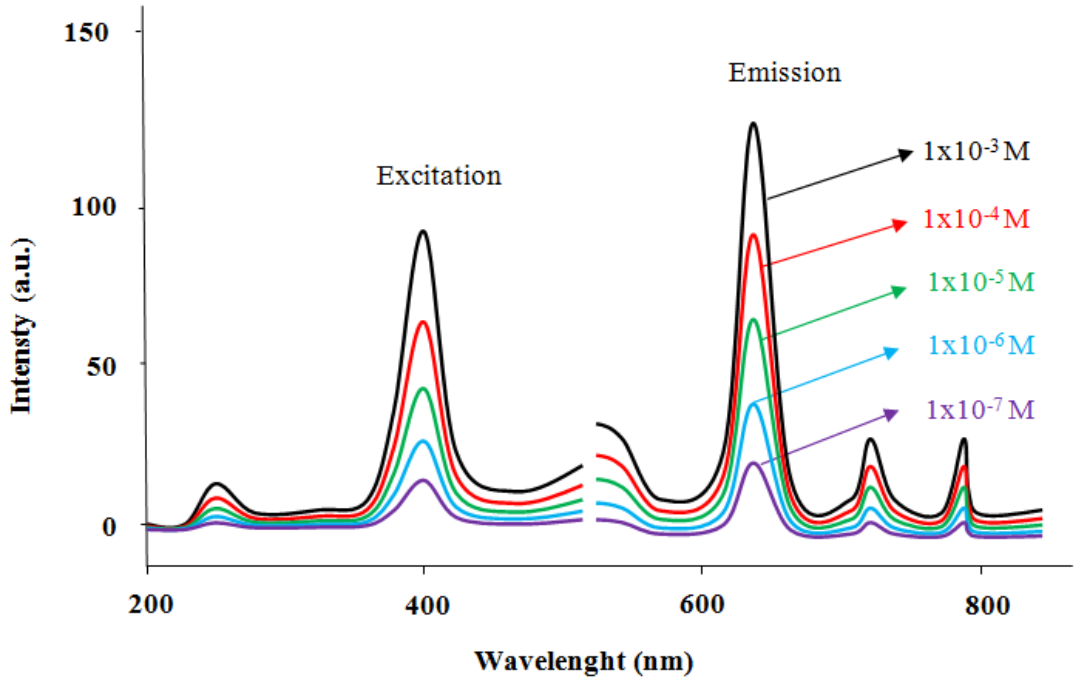

b) L^2 ($CHCl_3$)

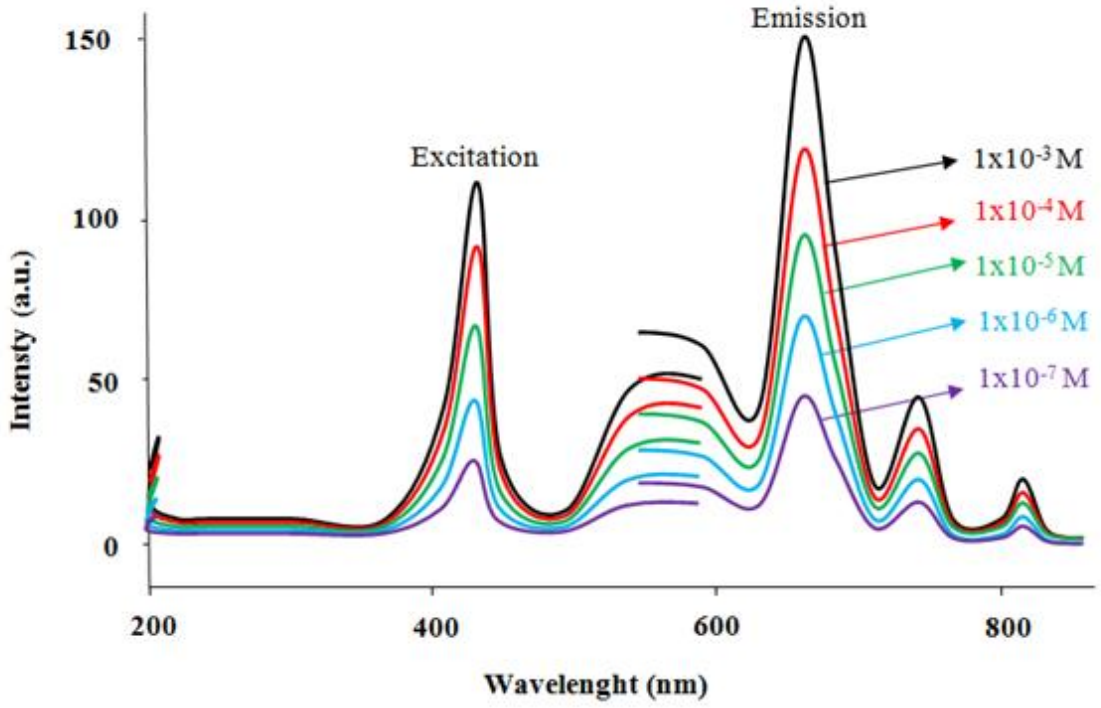

c) L^1 (C_2H_5OH)

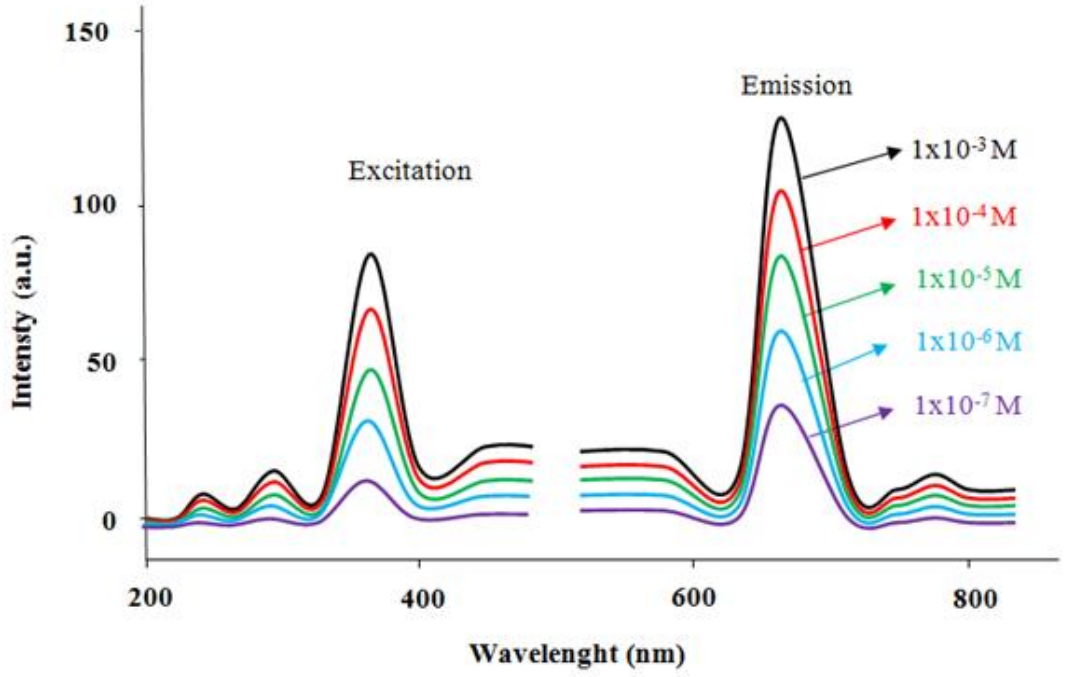

d) L^2 (C_2H_5OH)

Figs. 11a-d. Photoluminescence (excitation and emission) spectra of the imine compounds L^1 and L^2 in the different concentration and solvents.

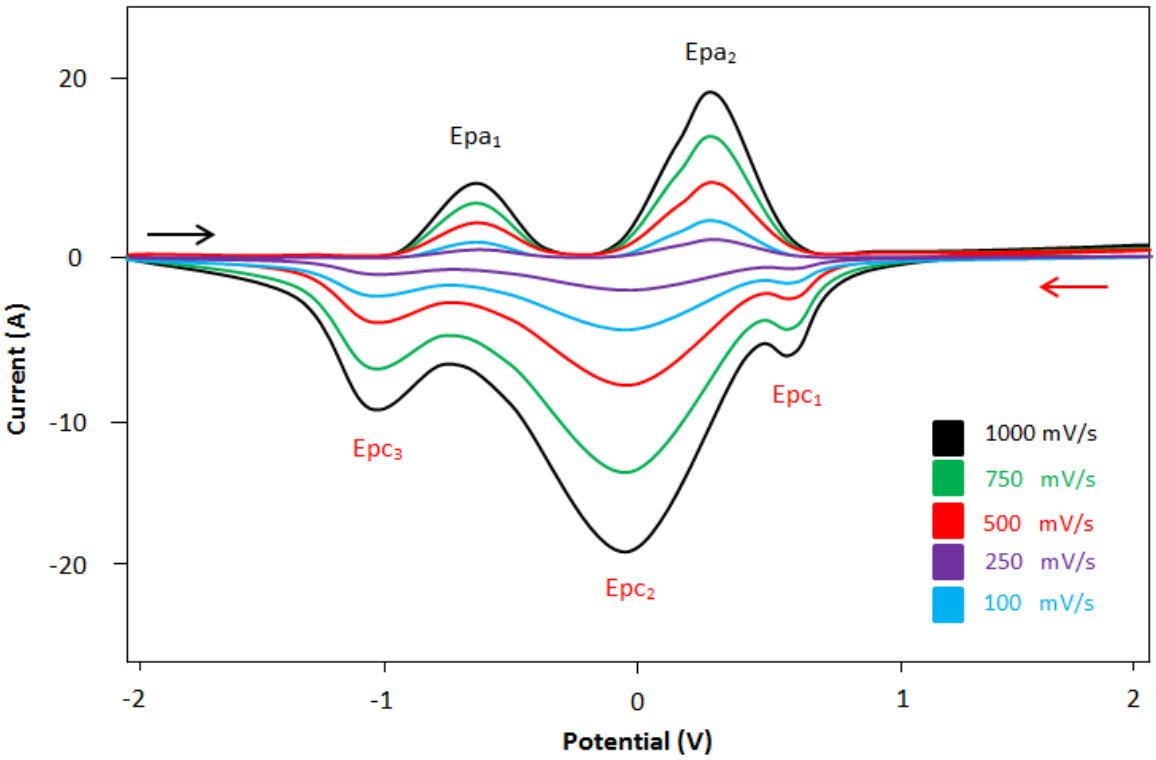

a) L^1, DMF ($1x\ 10^{-3}$ M)

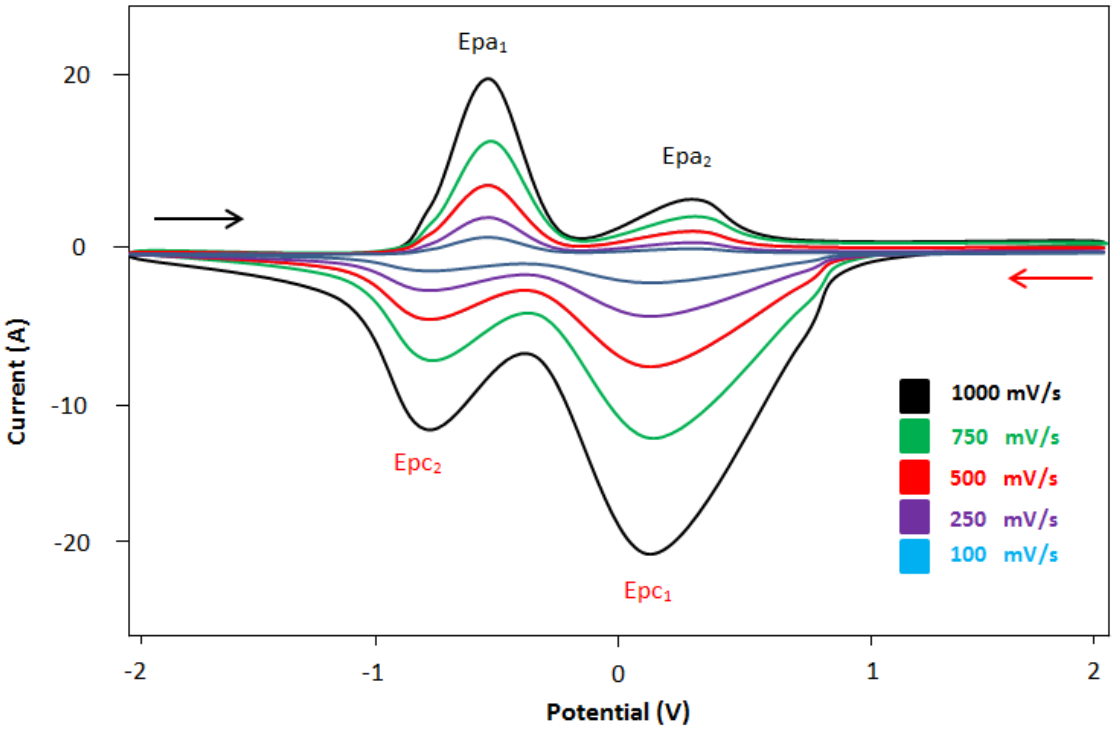

b) L^1, DMF ($1x\ 10^{-4}$ M)

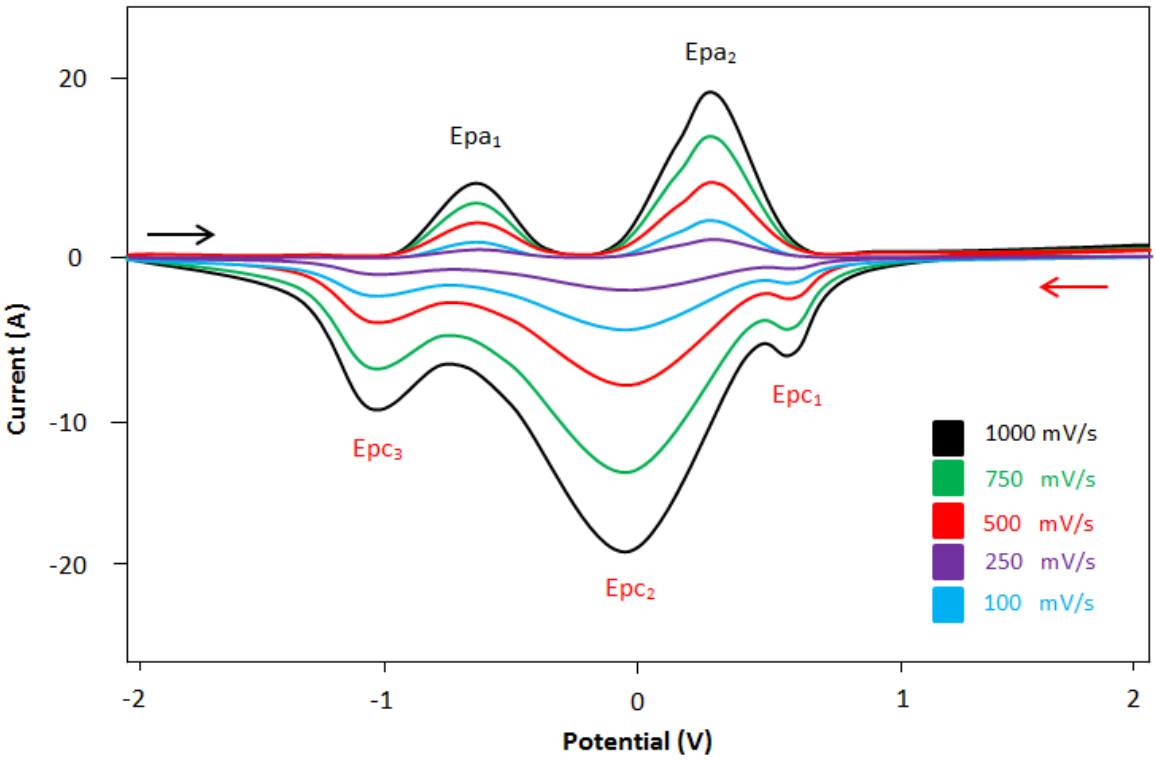

c) L^2, CH_3CN ($1x10^{-3}$ M)

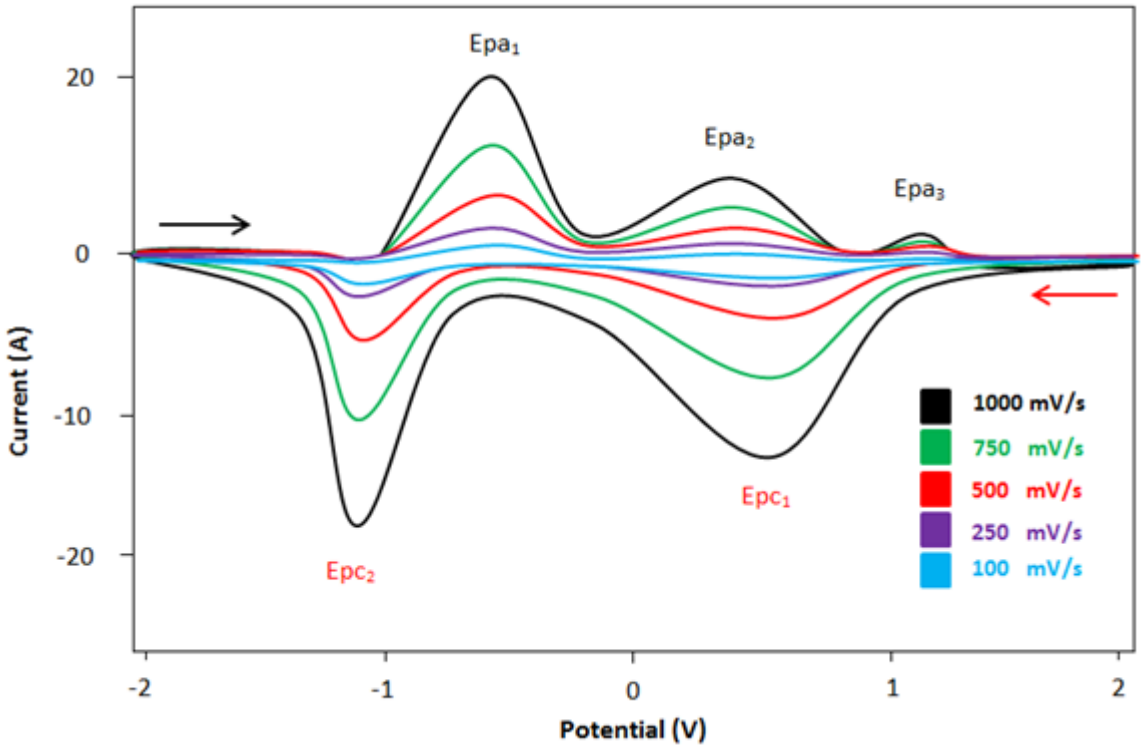

d) L^2, CH_3CN ($1x10^{-4}$ M)

Figs. 12a-d. CV curves of the imine compounds L^1 and L^2 in the different concentrations and solvents in the 100-1000 mV/s range.

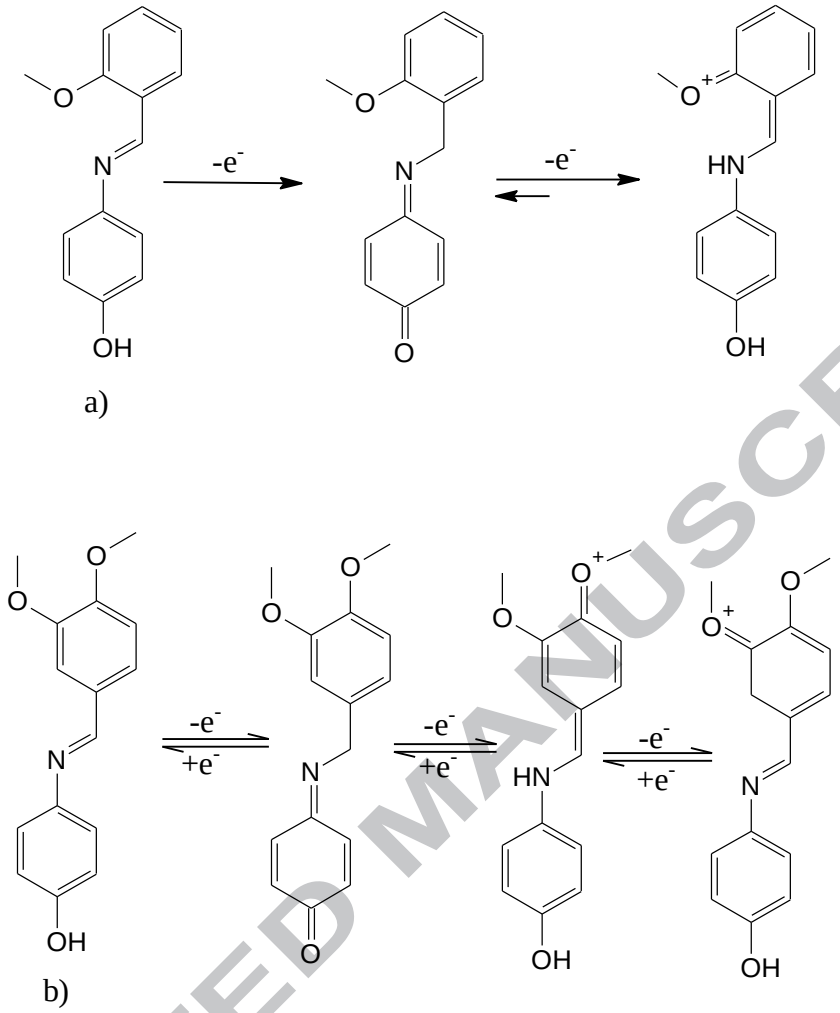

Figs. 13a,b. The proposed redox mechanism of the imine compounds L^1 (a) and L^2 (b) in the solution media.

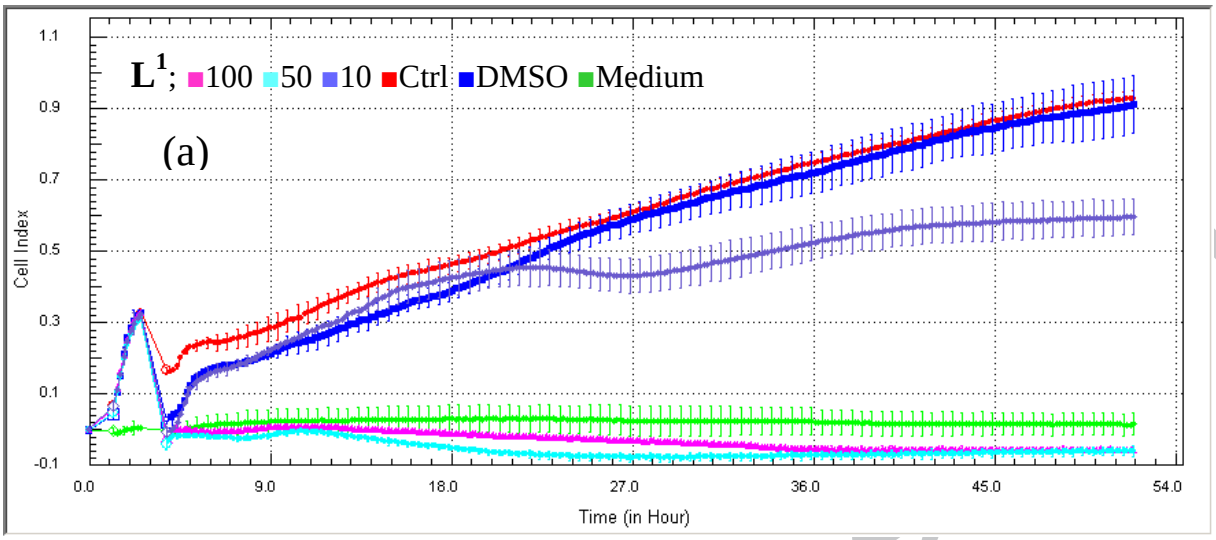

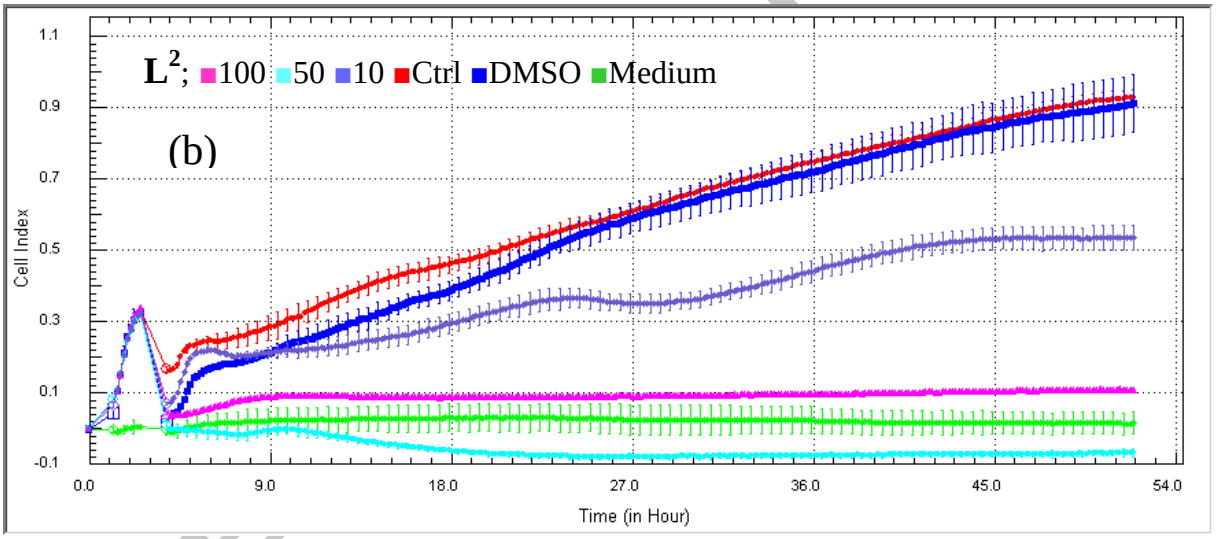

Figs. 14a,b. Anticancer activities of the imine compounds L^1 and L^2.

Table 1
UV-vis absorption spectral data of the imine compounds L^1 and L^2 in the different solvents.

	λ_{max} (ε_{max})									
	Methanol	Ethanol	$CHCl_3$	DMSO	DMF	n-hexane	n-heptane	Cyclohexane	Toluen	Dichloromethane
L^1	242($1.10x10^4$), 272($1.00x10^4$), 345($1.06x10^4$)	240($0.98x10^4$), 273($0.50x10^4$), 342($0.72x10^4$)	265($0.95x10^4$), 350($1.10x10^4$)	236($1.66x10^4$), 343($0.66x10^4$)	235($2.30x10^4$), 335($1.25x10^4$)	212($3.80x10^4$), 250($1.40x10^4$), 278($1.25x10^4$), 415($1.40x10^4$)	209($2.90x10^4$), 256($0.80x10^4$), 357($0.60x10^4$)	210($3.10x10^4$), 255($1.00x10^4$), 358($0.80x10^4$)	240($2.55x10^4$), 350($2.00x10^4$)	208($2.60x10^4$), 256($1.30x10^4$), 345($2.50x10^4$)
L^2	223($2.25x10^4$), 265($1.66x10^4$), 291($1.70x10^4$), 315($1.90x10^4$)	234($1.00x10^4$), 267($1.30x10^4$), 322($1.50x10^4$)	220($1.95x10^4$), 266($1.33x10^4$), 319($1.70x10^4$)	275($0.75x10^4$), 310($0.90x10^4$)	277($0.30x10^4$), 317($0.25x10^4$)	219($3.50x10^4$), 283($1.20x10^4$), 350($1.00x10^4$)	214($2.95x10^4$), 289($0.95x10^4$), 370($0.50x10^4$)	229($1.30x10^4$), 292($0.30x10^4$), 355($0.10x10^4$)	227($1.75x10^4$), 300($0.65x10^4$), 375($0.30x10^4$)	225($1.55x10^4$), 289($0.40x10^4$), 380($0.10x10^4$)

Table 2
Crystallographic data for the imine compounds L^1 and L^2.

Identification code		L^1	L^2
Empirical formula		$C_{14}H_{13}NO_2$	$C_{15}H_{15}NO_3$
Formula weight		227.25	257.28
Crystal size (mm^3)		0.55 x 0.25 x 0.22	0.80 x 0.25 x 0.10
Crystal color		Yellow	Yellow
Crystal system		*Monoclinic*	*Orthorhombic*
Space group		*P2(1)/c*	*Pna2(1)*
Unit cell	*a* (Å)	11.1980(7)	23.1187(13)
	b (Å)	17.2131(10)	12.4024(7)
	c (Å)	12.3101(7)	17.9426(10)
	α (°)	90	90
	β (°)	98.7710(10)°	90
	γ (°)	90	90
Volume (Å3)		2345.1(2)	5144.6(5)
Z		8	16
Abs. coeff. (mm^{-1})		0.087	0.093
Refl. collected		20498	44658
Completeness to θ = 26.43°		99.7 %	99.9 %
Ind. Refl. [R_{int}]		4809 [0.0164]	10554 [0.0455]
R1, wR2 [I>2σ (I)]		0.0334, 0.0834	0.0365, 0.0761
R1, wR2 (all data)		0.0384, 0.0875	0.0507, 0.0823
CCDC number		1034582	1034583

Table 3

Hydrogen bonds for the imine compound L^1 [Å and °].

D-H···A	d(D-H)	d(H···A)	d(D···A)	<(DHA)
O(2)-H(2A)···N(2)^{i}	0.870(17)	1.951(17)	2.8013(12)	165.3(15)
O(4)-H(4A)···N(1)	0.896(16)	1.861(17)	2.7480(12)	169.9(15)
C(5)-H(5)···O(4)	0.95	2.56	3.4496(15)	155.7
C(24)-H(24)···O(2^{ii}	0.95	2.56	3.4118(13)	149.2
C(19)-H(19)···O(2)^{i}	0.95	2.55	3.1566(14)	121.9

Symmetry transformations used to generate equivalent atoms: *i*: -x+1,-y+2,-z+1 *ii*: x,y,z+1

Table 4

Hydrogen bond parameters for the imine compound L^2 [Å and °].

D-H···A	d(D-H)	d(H···A)	d(D···A)	<(DHA)
O(6)-H(6)···N(1)	0.91(2)	1.97(2)	2.858(2)	165(2)
O(12)-H(12A)···N(3)	0.95(2)	1.80(2)	2.718(2)	161(2)
O(3)-H(3)···N(2)^{i}	0.91(2)	1.88(2)	2.775(2)	168(2)
O(9)-H(9A)···N(4)^{ii}	0.96(2)	1.84(2)	2.792(2)	169(2)
C(26)-H(26)···O(9)^{iii}	0.95	2.68	3.542(2)	151.2
C(60)-H(60)···O(9)^{iv}	0.95	2.45	3.221(2)	138.0
C(5)-H(5)···O(6)	0.95	2.70	3.566(2)	151.2
C(15)-H(15)···O(6)	0.95	2.53	3.299(2)	138.4

Symmetry transformations used to generate equivalent atoms: *i*: x+1/2,-y+1/2,z *ii*: x+1/2,-y+3/2,z *iii*: x-1/2,-y+1/2,z *iv*: x-1/2,-y+3/2,z

Table 5

Excitation and emission spectral data of the imine compound L^1 in both different concentration and solvents.

	(λ_{max})									
	DMF		DMSO		$CHCl_3$		Methanol		Ethanol	
	Excitation	Emission	Excitation	Emission	Excitation	Emission	Excitation	Emission	Excitation	Emission
$1x10^{-3}$	400, 475	620, 720	320, 395	660, 757, 825	405	660, 750, 830	395	665, 745, 805	430	660, 734, 813
$1x10^{-4}$	400, 475	619, 720	321, 396	660, 757, 825	405	660, 750, 830	430	660, 734, 813	430	660, 734, 813
$1x10^{-5}$	401, 476	619, 719	660, 757, 825	322,396	404	661, 751, 831	396	664, 744, 804	430	619, 735, 813
$1x10^{-6}$	401, 476	618, 719	322, 396	659, 756,	404	661, 751, 831	396	663, 743, 803	431	619, 735, 812
$1x10^{-7}$	402, 476	618, 719	323, 397	658, 755, 823	403	662, 752, 832	397	663, 743, 803	431	619, 735, 812

Table 6

Excitation and emission spectral data of the imine compound L^2 in both different concentration and solvents.

	(λ_{max})									
	DMF		DMSO		$CHCl_3$		Methanol		Ethanol	
	Excitation	Emission	Excitation	Emission	Excitation	Emission	Excitation	Emission	Excitation	Emission
$1x10^{-3}$	407	620, 690, 823	415	655, 760, 825	245, 400	635, 710, 777	245, 385	657, 745	240, 383, 363	665, 775
$1x10^{-4}$	407	620, 690, 823	416	655, 760, 825	245, 400	633, 710, 777	245, 285	657, 745	240, 283, 363	665, 775
$1x10^{-5}$	408	619, 689, 822	416	655, 761, 826	245, 400	635, 710, 777	245, 385	657, 745	665, 775	240, 283, 363
$1x10^{-6}$	408	619, 689, 822	417	654, 761, 826	245, 400	635, 709, 778	246, 386	656, 744	239, 282, 362	664, 774
$1x10^{-7}$	409	618, 688, 821	417	654, 762, 827	245, 400	633, 709, 778	246, 386	656, 744	239, 282, 362	664, 774

Table 7
The electrochemical data of the imine compounds L^1 and L^2 in both different concentration and solvents.

Compound	Solvent	Concentration (M)	Scan rate (mV/s)	E_{pa}(V)	E_{pc}(V)	I_{pa}/I_{pc}	$E_{1/2}$(V)	ΔE_p(V)
L1	ACN	$1x10^{-3}$	100	-0.75, -0.23, 1.09	0.70, -0.06	1.55	-	0.05
			250	-0.76, -0.24, 1.10	0.71, -0.07	1.54	-	0.05
			500	-0.77, -0.25, 1.11	0.72, -0.08	1.54	-	0.05
			750	-0.78, -0.26, 1.12	0.73, -0.09	1.52	-	0.05
			1000	-0.79, -0.27, 1.13	0.74, -0.10	1.52	-	0.05
	DMF		100	-0.80, 0.61	0.85, 0.05, -0.90	0.88	-	0.56
			250	-0.81, 0.62	0.86, 0.04, -0.91	0.89	-	0.58
			500	-0.82, 0.63	0.87, 0.03, -0.92	0.89	-	0.60
			750	-0.83, 0.64	0.88, 0.02, -0.93	0.89	-	0.62
			1000	-0.85, 0.65	0.89, 0.01, -0.94	0.90	-	0.64
	ACN	$1x10^{-4}$	100	-0.49, 1.11	0.61, 0.20, -1.00	1.81	-	0.50
			250	-0.48, 1.12	0.60, 0.21, -1.01	1.86	-	0.52
			500	-0.47, 1.13	0.59, 0.22, -1.03	1.91	-	0.54
			750	-0.46, 1.14	0.58, 0.23, -1.04	1.96	-	0.56
			1000	-0.45, 1.15	0.57, 0.24, -1.06	2.01	-	0.58
	DMF		100	-0.58, 0.26	0.18, -0.75	1.44	-	0.08
			250	-0.56, 0.27	0.16, -0.76	1.68	-	0.11
			500	-0.54, 0.28	0.15, -0.77	1.86	-	0.13
			750	-0.53, 0.29	0.13, -0.78	1.93	-	0.16
			1000	-0.51, 0.30	0.11, -0.79	2.30	-	0.19
L2	ACN	$1x10^{-3}$	100	-0.60, 0.37, 1.10	0.50, -1.12	0.74	-	0.60
			250	-0.61, 0.38, 1.11	0.51, -1.13	0.74	-	0.60
			500	-0.62, 0.39, 1.13	0.52, -1.14	0.75	-	0.61
			750	-0.63, 0.40, 1.14	0.53, -1.15	0.75	-	0.61
			1000	-0.64, 0.41, 1.15	0.55, -1.16	0.74	-	0.60
	DMF		100	-0.71, -0.25, 0.62	0,76, 0.30, -0.71	1.00	0.71	0.32
			250	-0.72, -0.26, 0.63	0.77, 0.31, -0.72	1.00	0.72	0.32
			500	-0.73, -0.27, 0.64	0.78, 0.32, -0.73	1.00	0.73	0.32
			750	-0.75, -0.28, 0.65	0.79, 0.33, -0.75	1.00	0.75	0.32
			1000	-0.76, -0.28, 0.67	0.80, 0.35, -0.76	1.00	0.76	0.32

continue								
L2	ACN	$1x10^{-4}$	100	-0.50, 0.20, 1.06	0.46, -0.11	0.43	-	0.60
			250	-0.52, 0.19, 1.07	0.47, -0.12	0.40	-	0.60
			500	-0.54, 0.19, 1.07	0.48, -0.14	0.39	-	0.59
			750	-0.55, 0.18, 1.08	0.50, -0.15	0.36	-	0.58
			1000	-0.56, 0.17, 1.09	0.51, -0.16	0.33	-	0.58
	DMF		100	-0.45, 0.47, 1.23	0.90, 0.46, -0.60	1.00	0.46	0.38
			250	-0.46, 0.48, 1.24	0.93, 0.47, -0.62	1.00	0.47	0.31
			500	-0.47, 0.49, 1.25	0.96, 0.48, -0.64	1.00	0.48	0.29
			750	-0.48, 0.49, 1.26	0.99, 0.49, -0.68	1.00	0.49	0.27
			1000	-0.49, 0.50, 1.27	1.00, 0.49, -0.69	1.00	0.49	0.27

All the potentials are referenced to Ag^{+}/AgCl; where E_{pa} and E_{pc} are anodic and cathodic potentials, respectively. $\Delta Ep = E_{pa} - E_{pc}$. $E_{1/2} = 0.5$ x ($E_{pa} + E_{pc}$).

Anticancer, photoluminescence and electrochemical properties of structurally characterised two imine derivatives

Gökhan Ceyhan[a], Muhammet Köse[a], Mehmet Tümer[a], İbrahim Demirtaş[b]

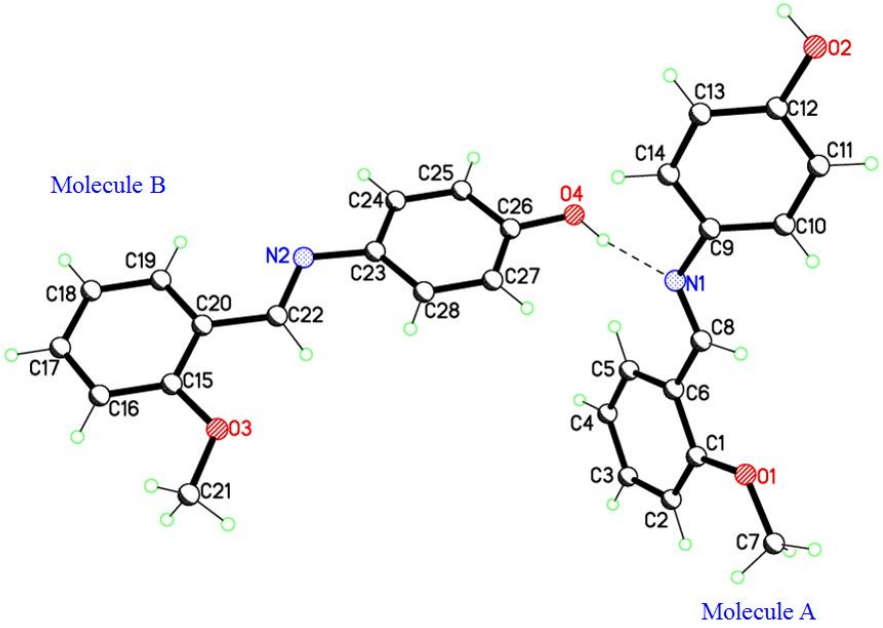

Fig. Molecular structure of the compound L^1 with atom numbering. Intra-molecular hydrogen bonding (OH···N) is shown as dashed lines.

Anticancer, photoluminescence and electrochemical properties of structurally characterised two imine derivatives

Gökhan Ceyhan[a], Muhammet Köse[a], Mehmet Tümer[a], İbrahim Demirtaş[b]

. Anticancer

. pholuminescence

. imine derivatives

. X-ray crystallography